



KASDI MERBAH OUARGLA UNIVERSITY



Faculty of New information and communication Technologies  
Department of Electronics and Telecommunications

MEMORY

# PRESENTED FOR THE GRADUATION OF MASTER

Specialty: Telecommunications

Option: Telecommunication Systems

By:

Abdelmonim Rezzag Lagra and Boulifa Aymen Anes

Theme:

*Automatic TM-CFAR Based on Artificial Neural  
Networks: Application on the Acquisition Stage  
of DS-CDMA Systems.*

*Before the jury composed of:*

Mr. AOUNALLAH  
Naceur

Prof

President

UKM Ouargla

Mr. MOAD Mohamed Sayah

MCA

examiner

UKM Ouargla

Mrs. BENKRINAH Sabra

MCB

Supervisor

UKM Ouargla

Mrs. OUERFELLA  
Elbahdja

PhD student

Co-supervisor

UKM Ouargla

academic year : 2023/2024

# بِسْمِ اللَّهِ الرَّحْمَنِ الرَّحِيمِ

## Thanks :

First and foremost, we thank Almighty God. It is through His grace that we have had the courage and strength to accomplish this work.

We would like to express our profound gratitude and respect to Mrs. Benkrinah Sabra and Dr. Ourfella El Bahdja for their invaluable help and constant encouragement throughout this work.

Special thanks to the discussion committee members for their support.

We also extend our thanks to all the professors of the Electronics and Telecommunications Department who have contributed to our development and enabled us to reach this stage in our academic journey.

Additionally, we would like to thank our families for their unwavering support and encouragement throughout our educational journey, from childhood to the present day.

Finally, we thank all our friends we have met through our studies and beyond, who have contributed to our success and encouraged us to continue our path and achieve our goals.

**Thank you all**

**List of abbreviations :**

ATM-CFAR	Automatic Trimmed-Mean-CFAR
AWGN	Additive White Gaussian Noise
CA-CFAR	Cell Averaging Constant False Alarm Rate
CDMA	Code Division Multiple Access
CFAR	Constant False Alarm Rate
CMLD-CFAR	Censored Mean Level Detectors CFAR
CUT	Cellule Under Test
DS-CDMA	Direct Sequence-Code Division Multiple Access
FDMA	Frequency Division Multiple Access
FH-CDMA	Frequency Hopping-Code Division Multiple Access
GO-CFAR	Greatest Of –CFAR
MGF	Moment Generating Functions
MNN	Memory Network Neuronal
NN	Neural networks
OS-CFAR	Ordered Statistics CFAR
PN	Pseudo-Noise
RF	Radio Frequency
(PLL)	Phase-Locked Loop
SFH-CDMA	Slow Frequency Hopping-CDMA
SNR	Signal to Noise Ratio
SO-CFAR	Smallest OF-CFAR
TDMA	Time Division Multiple Access
TM-CFAR	Trimmed Mean-CFAR

**List of figures :**

Fig (I.1): Illustration of propagation mechanisms ..... 4

Fig (I.2): Time multiplexing (TDMA) scheme ..... 6

Fig (I.3): Diagram of a frequency multiplexing (FDMA) scheme..... 6

Fig (I.4): Code division multiple access (CDMA) scheme ..... 7

Fig (I.5): Spreading a data sequence..... 9

Fig (I.6): General diagram of a DS spreading system..... 9

Fig (I.7): General acquisition circuit..... 11

Fig (I.8): Principle of serial acquisition..... 11

Fig (I.9) : Parallel acquisition principle ..... 12

Fig (I.10): Hybrid acquisition principle..... 13

Fig (I.11) Block diagram of an adaptive detection system..... 14

Fig (I.12) Block diagram of conventional CFAR detectors..... 14

Fig (I.13) Functional diagram of the detector OS-CFAR..... 15

Fig (I.14) Block diagram of the detector CMLD-CFAR ..... 16

Fig (I.15) Functional diagram of the detector TM-CFAR..... 16

Fig (II.1) Scheme of the proposed system ..... 20

Fig (II.2) Correlator consist of in-phase (I) and quadrature-phase (Q) components..... 24

Fig (II.3): Example of an MLP network ..... 27

Fig (II.4) Random Search Algorithm.....29

Fig (III.1): Database training using the MLP network.....32

Fig (III.2): Probability of detection ( $P_d$ ) by reference to noise ratio for each segment (SNR/Chip) for different detection sections ( $r$ ).....33

Fig (III.3): Time of acquisition ( $T_{aq}$ ) indicating the ratio of signal to noise per sector (SNR/Chip) for different detection sections ( $r$ ).....33

Fig (III.4): Probability of detection ( $P_d$ ) by reference to noise ratio per chip (SNR/Chip) for different code lengths ( $N$ ).....**34**

Fig (III.5): Time of acquisition ( $T_{aq}$ ) denotes noise ratio per chip (SNR/Chip) for different code lengths ( $N$ ).....**34**

Fig (III.6): Probability of detection ( $P_d$ ) by reference to noise ratio per chip (SNR/Chip) for different false alarm probability ( $P_{fa}$ ).....**36**

Fig (III.7): Time of acquisition ( $T_{aq}$ ) denotes noise ratio per chip (SNR/Chip) for different false alarm probability ( $P_{fa}$ ).....**36**

Fig (III.8): Probability of detection ( $P_d$ ) by reference to noise ratio per chip (SNR/Chip) for different effect of power ratio ( $\rho$ ).....**37**

Fig (III.9): Time of acquisition ( $T_{aq}$ ) denotes noise ratio per chip (SNR/Chip) for different effect of power ratio ( $\rho$ ).....**37**

**Table of contents :**

Thanks.....	<b>I</b>
List of abbreviations .....	<b>II</b>
List of figures .....	<b>III</b>
Table of contents .....	<b>V</b>
General Introduction.....	<b>2</b>
<b>Chapter I: Basic Concepts on propagation phenomena and detection techniques</b>	
I-1 Introduction .....	<b>4</b>
I-2 RF Wave .....	<b>4</b>
I-3 Concept on Propagation Phenomena.....	<b>4</b>
I-4 Phenomenon of Multipath .....	<b>5</b>
I-4-1 Positive Effect of Multipath.....	<b>5</b>
I-4-2 Negative Effect of Multipath.....	<b>5</b>
I-5: Frequency Shift (Doppler Shift) .....	<b>5</b>
I-6 : Network Access Methods.....	<b>5</b>
I-6-1: Time Division Multiple Access (TDMA).....	<b>5</b>
I-6-2: Frequency Division Multiple Access (FDMA).....	<b>6</b>
I-6-2: Code Division Multiple Access (CDMA).....	<b>7</b>
I-6-1-1 CDMA Advantages.....	<b>7</b>
I-6-1-2 CDMA Disadvantages.....	<b>7</b>
I-6-2 CDMA Characteristics.....	<b>7</b>
I-6-3 CDMA Principle.....	<b>7</b>
I-7 Spectrum Spreading Technique.....	<b>8</b>
I-7-1 Principle Of Spread Spectrum.....	<b>8</b>
I-8 Direct Sequence Spectrum Spread (DS-SS) .....	<b>9</b>
I-8-1 Advantages.....	<b>10</b>
I-8-2 Disadvantages.....	<b>10</b>
I-9 Synchronization in DS-CDMA Systems.....	<b>10</b>
I-10 Acquisition Phase.....	<b>10</b>
I-11 Strategies Search.....	<b>11</b>

I-11-1 Serial Search.....	11
I-11-2 Parallel Search.....	12
I-11-3 Hybrid Search .....	12
I-12 CFAR Detection .....	13
I-12-1 CA-CFAR.....	14
I-12-2 GO-CFAR .....	15
I-12-3 OS-CFAR .....	15
I-12-4 CMLD-CFAR.....	15
I-12-5 TM-CFAR.....	16
I-12-6 ATM-CFAR .....	16
I-13 Conclusion .....	17
<b>Chapter II: Description of Neural Network ATM-CFAR Detector.</b>	
II-1 Introduction .....	19
II-2 Application of ATM-CFAR to Adaptive PN Sequence Acquisition.....	21
II-2-1 Description of the Proposed System.....	21
II-3 System Description and Problem Formulation.....	21
II-3-1 Received Signal Model.....	22
II-3-2 Correlator.....	23
II-3-3 ATM-CFAR Detector.....	25
II-3-4 Neural Networks.....	27
II-3-4-1 MLP Networks.....	27
II-4 Learning algorithms .....	28
II-4-1 Supervised learning .....	28
II -5 Backpropagation algorithm.....	28
II -6 Random Search Method (Monte Carlo Method).....	28
II-7 Analysis of the Proposed System.....	29
II-7-1 Decision Variables.....	29
II-7-2 Detection and False Alarm Probabilities.....	30
II-7-3 Mean Asquisition Time.....	30
II-8 Conclusion.....	30

**Chapter III Results and Discussions**

III.1 Introduction.....32

III.2 Results and Discussions.....32

    III.2.1 Effect of interfering cell number ( $r$ ).....33

    III.2.2 Effect of Partial Correlation Length ( $N$ ).....34

    III.2.3 Effect of False Alarm Probability ( $P_{fa}$ ).....35

    III.2.4 Effect of Power Ratio ( $\rho$ ).....37

III.3 Conclusion.....38

General Conclusion.....40

References.....43

Abstract .....45



# **General Introduction:**

Recently, the interest in Direct Sequence Code Division Multiple Access (DS/CDMA) for mobile transmissions has significantly increased. In DS/CDMA systems, recovering the transmitted information requires despreading the received signal using a locally generated pseudo-random code (PN). This necessitates precise synchronization between the received codes and the locally generated ones before data detection. Therefore, rapid establishment of code synchronization is a crucial issue in DS/CDMA systems.

The synchronization process generally occurs in two stages: acquisition and tracking. Acquisition involves coarse synchronization of the received sequence with the locally generated sequences to within a fraction of chip duration (the bit duration of the PN sequence). The second stage, tracking, ensures fine alignment of the sequences, allowing the receiver to determine the start and end of each symbol.

In mobile systems, information transmission over the radio link can occur from a base station to a mobile device (downlink) or from a mobile device to a base station (uplink). Propagation conditions vary significantly depending on the environment, often necessitating initial code acquisition in highly degraded conditions. These environments may include very low signal-to-noise ratios, the presence of jammers, channel fading, and multi-access interference, making received signal levels unpredictable.

Fixed threshold techniques are not suitable in such contexts due to the high risk of false alarms. Therefore, it is essential to use adaptive techniques, where the threshold is determined based on the ambient noise power. Many Constant False Alarm Rate (CFAR) processors used in radar systems have also been applied to PN sequence acquisition problems in DS/CDMA systems to combat the variability and instability of the detection ( $P_d$ ) and the false alarm ( $P_{fa}$ ) probabilities.

The objective of this study is to acquire PN sequences using an adaptive threshold through the ATM-CFAR (Automatic Trimmed Mean-CFAR) using artificial neural network techniques in non-homogeneous environments. This algorithm ensures better performance in terms of detection probability, even in challenging propagation conditions

# **Chapter I**

## **Concepts on propagation phenomena and detection techniques**

## I-1 Introduction:

In this chapter, we will introduce the basic concepts of RF (Radio Frequency) communication and various phenomena related to the propagation of electromagnetic waves, methods of accessing networks, and the technique of spectrum spreading. Then, we will focus on several types of CFAR detectors.

## I-2 RF Wave:

The RF wave propagates through space in various directions and may encounter a number of obstacles. The different obstacles constituting the propagation medium allow the emitted wave to take multiple paths before reaching the receiving antenna. Each path follows a different trajectory with its own delay, phase, amplitude, and arrival angle. The received signal is the combination of these multiple paths. This phenomenon of multipath can limit the transmission speed in wireless networks. When encountering an obstacle, some of the energy of this radio wave is absorbed, some may be reflected, and some continue to propagate with attenuated power. This results in four main categories of phenomena that affect signal propagation: reflection, diffraction, scattering, and dispersion [1].

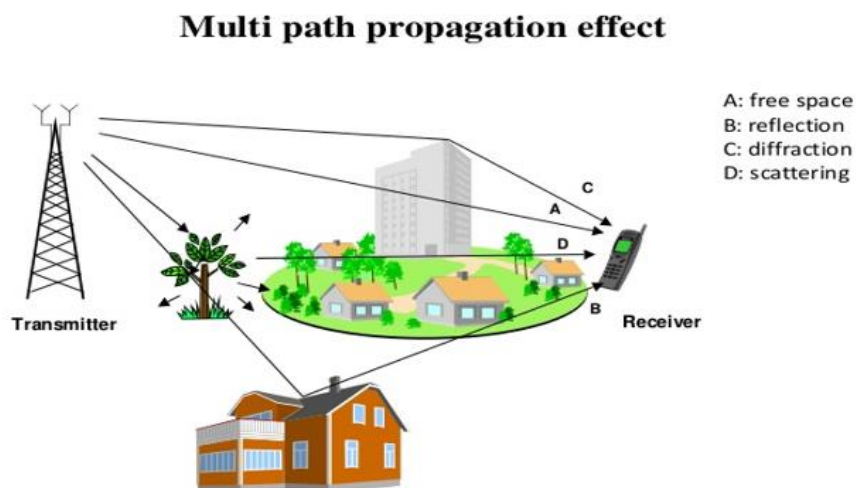


**Fig. I-1:** Illustration of propagation mechanisms.

## I-3 Concept on Propagation Phenomena :

- **Reflection:**

This phenomenon occurs when an electromagnetic wave encounters a smooth surface, whose dimensions are much larger than the wavelength of the signal [1].

- **Scattering:**

When the wave collides with an irregular surface or a surface whose dimensions are on the order of the wavelength, the reflected energy is scattered in all directions [1].

- **Diffraction:**

When the path of the wave between the transmitter and the receiver is obstructed by a large-bodied object with dimensions much larger than the wavelength, secondary waves are formed behind the object [1].

- **Dispersion:**

It occurs when the wave encounters a non-smooth, multi-angle surface. This phenomenon occurs when a wave encounters a multitude of obstacles per unit volume with dimensions of the same order of magnitude or smaller than the wavelength  $\lambda$ . In this case, the incident wave is reflected in multiple directions with different attenuations [1].

#### **I-4 Phenomenon of Multipath:**

In a wireless communication system, the system's environment interferes with the transmitted wave through various mechanisms. The receiver may receive the wave reflected off surfaces such as the ground, buildings, ... etc. These replicas are more or less delayed depending on the path lengths and more or less attenuated depending on the distance travelled and encountered propagation phenomena. They combine at the receiver in a constructive or destructive manner, giving rise to fading [2].

##### **I-4-1 Positive Effect of Multipath:**

Multipath propagation enables communication in cases where the transmitter and receiver are not in direct line of sight. When this condition is met, multiple paths allow radio waves to overcome obstacles to ensure some continuity of radio service [2].

##### **I-4-2 Negative Effect of Multipath:**

Multipath propagation presents several drawbacks, the most significant of which are:

a) *Delay spread*: In the channel, each path passes with different lengths. Thus, associated signals arrive with different delays [2].

b) *Rayleigh fading*: Rayleigh fading occurs when the signal envelope varies. The channel transmits to the receiver a large number of multipath signals. Constructive interference of this phenomenon occurs when multiple received signals add up and produce a resulting signal stronger than the signal from the direct path alone.

#### **I-5 Frequency Shift (Doppler Shift) :**

The movement of the transmitter or the receiver introduces spreading in the frequency domain, known as Doppler shift. If  $F_m$  represents the maximum Doppler shift, the Doppler spectrum bandwidth is given by:  $B_d = 2F_m$ . [2]

#### **I-6 Network Access Methods:**

The three main multiple access methods used in communication systems are Frequency Division Multiple Access (FDMA), Time Division Multiple Access (TDMA), and Code Division Multiple Access (CDMA) [3].

### 1-6-1 Time Division Multiple Access (TDMA):

In TDMA systems, the bandwidth is shared among all users, but the division occurs in the time domain. A carrier frequency is shared among different subscribers in time slots. Most TDMA-based radio frequency systems are synchronous, meaning they allocate transmission periods to each user to avoid multiple access interference (MAI). Each signal requires a specific time interval allocated to it, and the receivers also adhere to the associated intervals to reconfigure the sequence of information as we observe in Figure (I-2).

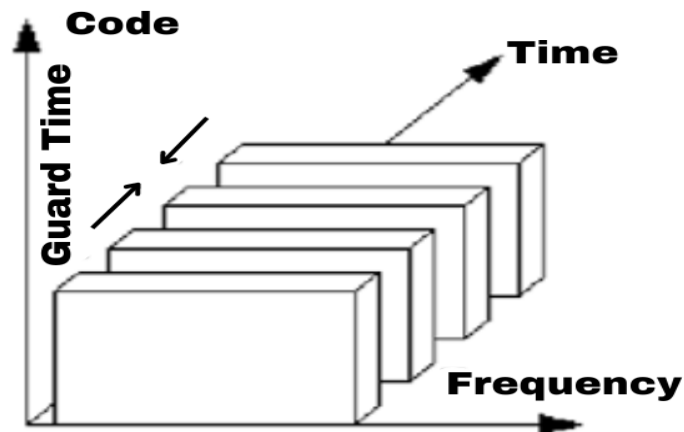


Fig.I-2: Time multiplexing (TDMA) scheme.

### I-6-2 Frequency Division Multiple Access (FDMA):

Frequency Division Multiple Access (FDMA) is a widely used multiplexing technique in radio frequency communication systems. It is considered the oldest multiple access method. FDMA involves dividing the channel bandwidth into  $U$  (number of users) bands of non-overlapping frequencies. Users transmit their signals continuously, with each signal being transmitted on a different frequency, as illustrated in Figure (I-3) [3].

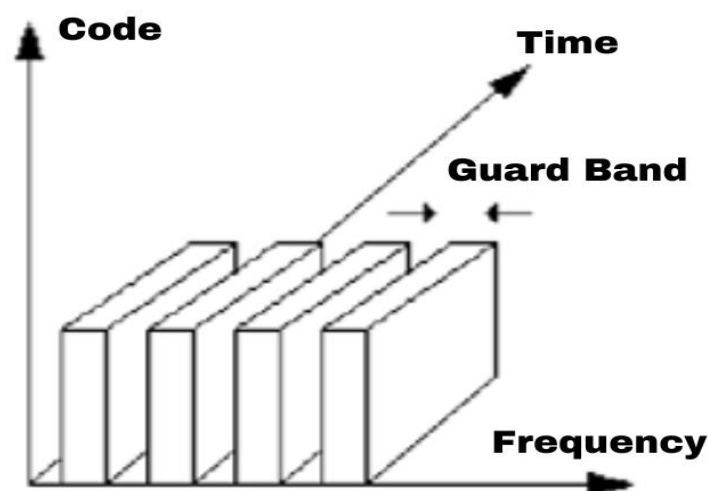
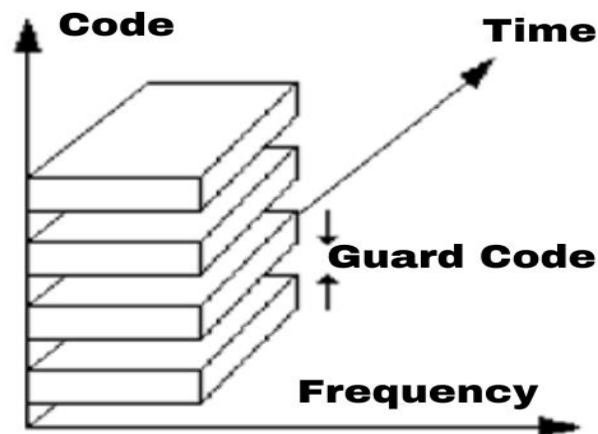


Fig.I-3: Diagram of a frequency multiplexing (FDMA).

### I-6-3 Code Division Multiple Access (CDMA):

Code Division Multiple Access (CDMA) is a more recent multiplexing technique compared to TDMA and FDMA. In this technique, users share the same frequency space and transmit over the same time intervals, as depicted in Figure (I-4). Spread spectrum technique is used to assign each user a unique code or sequence, which determines the frequencies and powers used [3].



**Fig.I-4:** Code Division Multiple Access (CDMA) Schema [4].

#### I-6-1-1 CDMA Advantages:

- Excellent protection against noise and interference.
- Greater flexibility compared to the other two techniques (TDMA and FDMA).
- Wide coverage.
- Frequency diversity.

#### I-6-1-2 CDMA Disadvantages:

- Time synchronization of codes is difficult.
- The transmission rate may be affected if all codes are used in the same system due to potential code interference and increased noise.

#### I-6-2 CDMA Characteristics:

The main characteristics of this type of system are as follows [4]:

- High frequency utilization: 7 to 10 times higher than current analog and TDMA/FDMA systems.
- Larger coverage area: up to a radius of 30 km.
- Universal frequency reuse: shared use of a single frequency band by all cell sites.
- Interference reduction: strong resistance to noise, packet transmission.

#### I-6-3 CDMA Principle:

The rapid rise of digital communication systems has contributed to the development of personal communication systems and cellular mobile radio systems such as wireless telephony. This has led to a

significant increase in the number of users, each with different transmission rates, who must share the same resources of such a system to access the same network for various services. Hence, the need for a more efficient multiple access technique, namely CDMA is necessary. In a CDMA system, the signal from each user is spread by its own spreading code and then transmitted through the radio channel. At the receiver, the received signal is despread by the same spreading code used at the transmitter to recover the originally transmitted data.

CDMA system based on spread spectrum not only improves the capacity of the communication system but also enables effective management of the available frequency band. Spread spectrum technique in CDMA is utilized by various methods. The most commonly used methods are FH-CDMA (Frequency Hopping-CDMA) and DS-CDMA (Direct Sequence-CDMA) [4].

*a) FH-CDMA (Frequency Hopping-CDMA):* In frequency hopping CDMA, data is transmitted on different frequencies that change periodically. This change indicated by the spreading code. There are two types of frequency hopping CDMA:

- 1- Slow Frequency Hopping (SFH-CDMA): Multiple code sequences are transmitted at the same frequency.
- 2- Fast Frequency Hopping (FFH-CDMA): Chips of the same code are transmitted over multiple frequencies.

*b) DS-CDMA (Direct Sequence-CDMA):* In DS-CDMA systems, data is encoded directly.

## **I.7 Spectrum spreading technique:**

Emerging in the 1940s thanks to the information theory developed successively by N. Wiener and C.E. Shannon, spread spectrum techniques were initially intended for secure digital communications such as military telecommunications. With the rise of mobile radio-communication systems, spread spectrum techniques have become prevalent in various standards such as *IS – 95, UMTS, IEEE802.1* [5].

### **I-7-1 Principle of Spread Spectrum:**

Spread spectrum is, by definition, a means of transmitting a given signal using a much wider frequency band than that employed by conventional techniques, utilizing a code sequence. The properties of such transmission system are numerous. Figure (I-5) illustrates a schematic example of spreading a data signal. The data signal, with a symbol duration of  $T_s$ , is multiplied by the spreading sequence with a chip rate of  $T_c$ . The ratio  $T_s/T_c$  is called the spreading factor  $G$ . At the receiver, the signal is multiplied by the code and integrated (correlated) to retrieve the transmitted information [5].



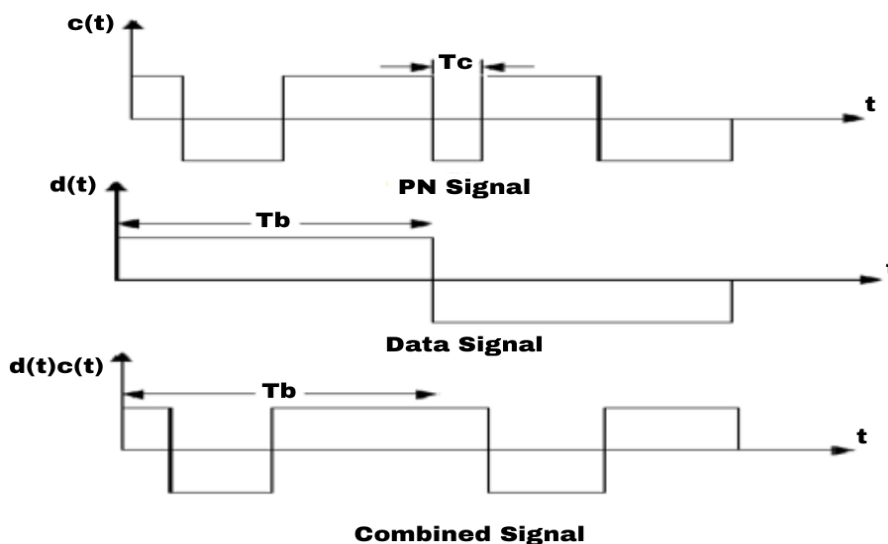


Fig.I-5: Spreading a data sequence.

### I-8 Direct Sequence Spread Spectrum (DS-SS):

Spread Spectrum by Direct Sequence (DS-SS) is the most widely used technique. It involves multiplying the transmitted information message, with a rate  $R_b$ , by a pseudo-random code with a lower rate,  $R_c$ . The ratio between the two defines the spreading gain:  $G = R_c / R_b$ , thus

$$G = T_b / T_c \tag{I-1}.$$

Where:

- $T_b = 1 / R_b$  is the duration of a chip bit.
- $G$  is usually an integer greater than 1 since it measures spectrum spreading and represents the number of chips per information bit.
- $T_c = 1 / R_c$  is the duration of a rectangular pulse of the code, also known as the information bit. This ratio is also referred to as the processing gain. In this sense, it represents a measure of resistance to interference and intentional jamming achieved by increasing the bandwidth of the transmitted signal [1,5].

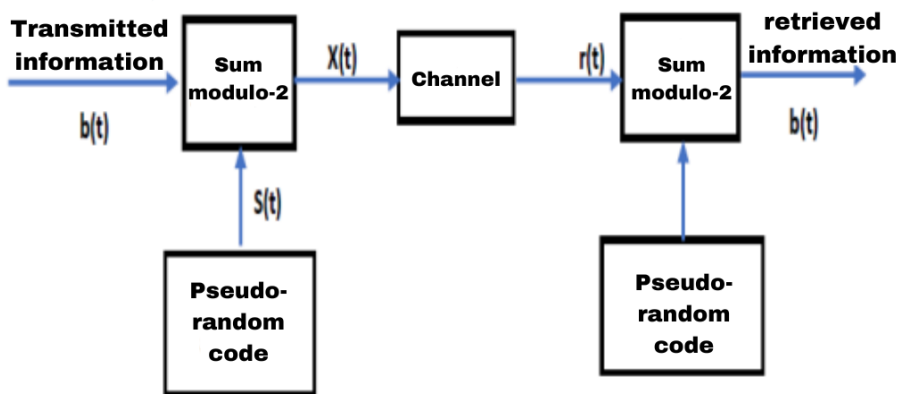


Fig.I-6: General diagram of a DS spectrum spreading system [5].

### **I-8-1 Advantages:**

- Utilization of a single carrier providing a simple frequency generator.
- DS-CDMA exhibits high resistance to multipath fading. In this case, interference between different paths is reduced.
- The increase in the number of users depends only on the number of codes used, not on the capacity of the radio channel, which remains limited and scarce.
- Robustness against jammers.

### **I-8-2 Disadvantages:**

- The spectral efficiency of DS-CDMA is low: the useful data rate per user is low compared to the occupied bandwidth.
- DS-CDMA is susceptible to near-far effect: signals from users closest to the base station, and thus received with high power levels, interfere with the weaker signals from distant users.  
A power control mechanism must be implemented to adjust the power levels of users based on their distance from the base station.

### **I-9 Synchronization in DS-CDMA Systems:**

Synchronization is a crucial task in direct sequence spread spectrum systems and is carried out in two stages: acquisition, which is the initial synchronization, and tracking, which is precise synchronization. Acquisition is the most important and the most challenging task. It synchronizes the received code with the locally generated code with a certain level of accuracy. Compared to acquisition, code tracking is a relatively simple task to accomplish; it can be performed using a Phase-Locked Loop (PLL). [6]

### **I-10 Acquisition Phase:**

The primary goal of PN code acquisition is to achieve coarse synchronization between the transmitter and the receiver. This is achieved by multiplying the received signal by shifted versions of the local code. A detector is used to perform this operation. Each relative position between the codes (of the transmitter and the receiver) is called a "cell." The total number of cells needed to verify the acquisition is called the "uncertainty region." This region is explored using a procedure known as a search strategy. PN code acquisition is a closed-loop process controlled by the search strategy block.

The purpose of acquisition is to synchronize the locally generated code with the received code. In this section, we will introduce various techniques used to achieve this alignment. They are all based on the principle described in Figure (I-7). The receiver assumes a phase for the spreading sequence and tries to despread the received signal using this same phase. If the proposed phase matches the sequence of the received signal, the wideband signal will be correctly despread, providing the original narrowband

information. A bandpass filter with a bandwidth similar to that of the narrowband signal is then used to recover the energy of the signal. Since the proposed phase is equal to that of the received signal, the bandpass filter will collect all the energy. In this case, the receiver concludes that coarse synchronization is achieved and activates the tracking loop to perform fine synchronization. Otherwise, if the proposed phase differs from that of the received signal, the bandpass filter will only recover a small portion of the energy. The receiver then concludes that the proposed phase is incorrect and retries with other phases .

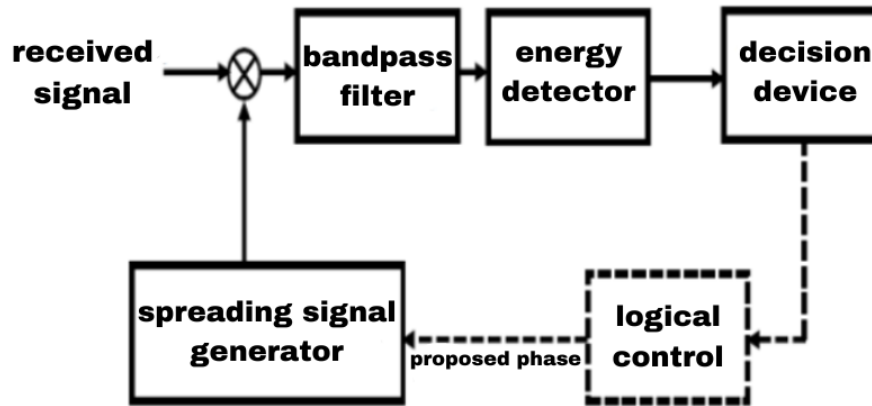


Fig.I-7: General Acquisition Circuit [6].

### I-11 Search Strategies:

Acquisition methods can be classified according to the approved search strategy into three systems: Serial, Parallel, and Hybrid.

#### I-11-1 Serial Search:

In this method, the acquisition circuit cycles through to test all possible phases, one after the other (in series), as shown in Figure (I-8). This type of circuit is not too complex. However, the time penalty associated with a missed hit is significant. Additionally, a longer integration time must be chosen to reduce the probability of misses. This results in a relatively long acquisition time [2].

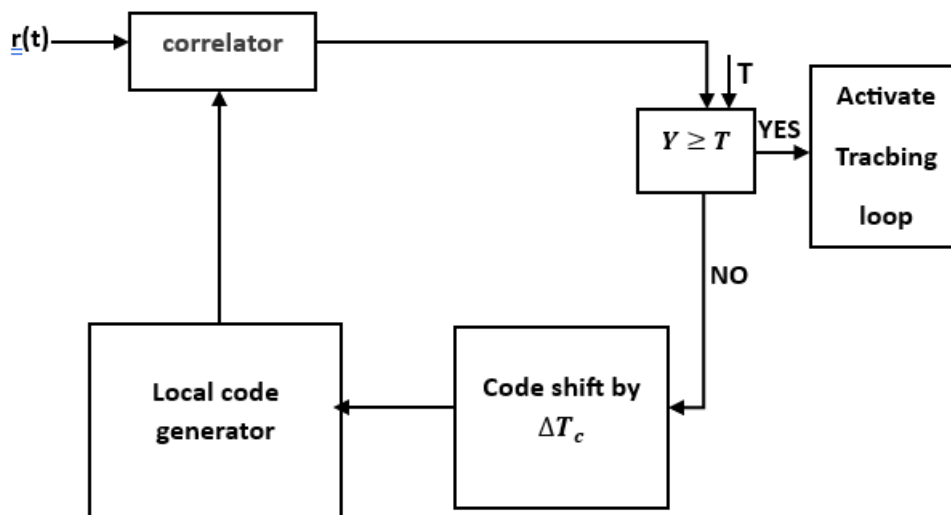
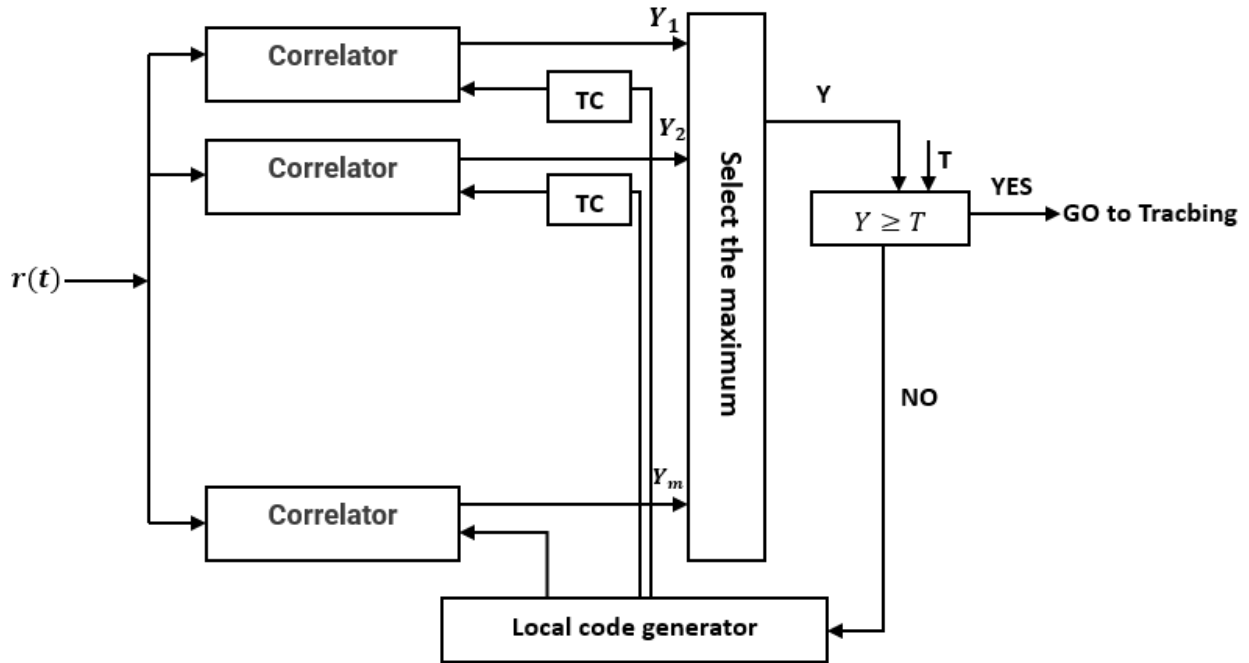


Fig.I-8: Principle of serial acquisition [2].

#### I-11-2 Parallel Search:

In a fully parallel acquisition system, the code acquisition time can be significantly reduced compared to the first technique, so that all code test phases are simultaneously tested, as shown in Figure (I-9). Although this technique is more complex than the first strategy, it allows for the generation of exceptionally long PN codes. This is because the simultaneous placement of multiple detectors maximizes the number of obtainable PN codes[2].



**Fig.I-9:** Parallel acquisition principle.

### I-11-3 Hybrid Search:

A hybrid search results from a mixture of the two previous methods (serial and parallel searches). The goal is to reduce the acquisition time of the first technique and the complexity of the devices in the second method. In case of lack of synchronization, the search phase is updated by  $N$  cells until synchronization is detected [2].

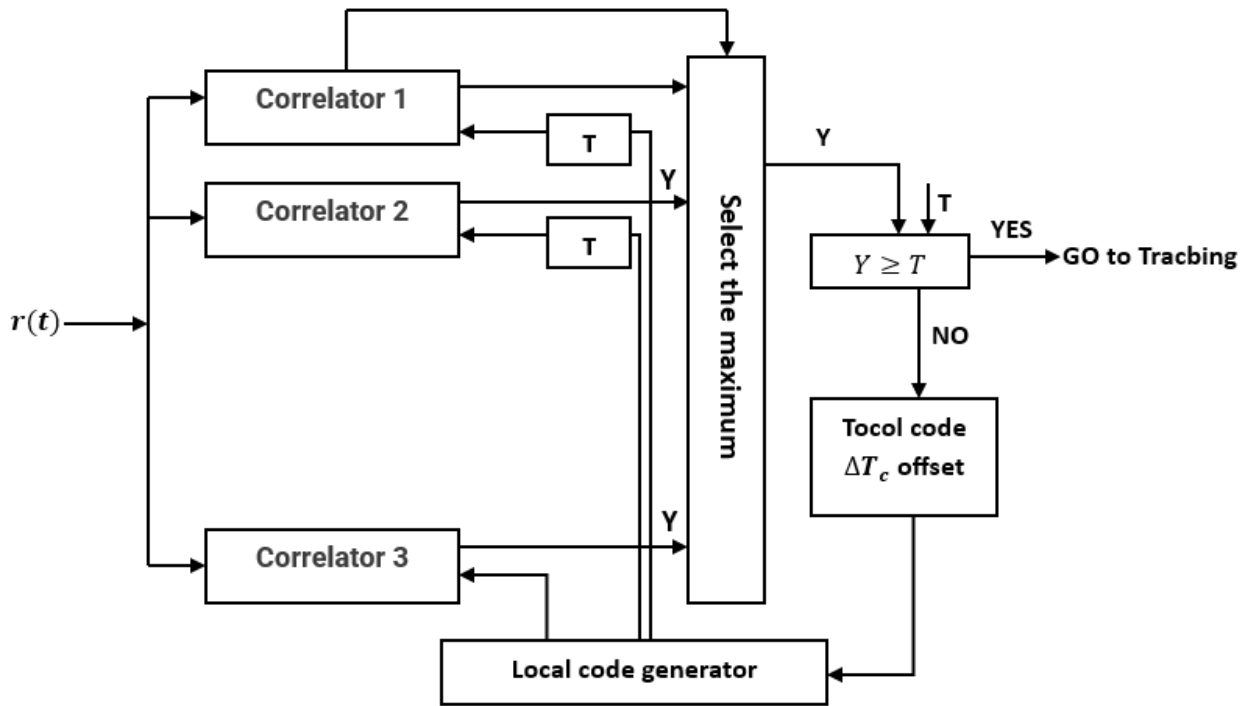


**Fig.I-10:** Hybrid acquisition principle [2].

### I-12 CFAR Detection:

CFAR algorithms operate by deriving a threshold from the probability density function (pdf) of the non-coherent detector's output signal under the null hypothesis  $H_0$ , which assumes that no target is present in the detection cell. This threshold, crucial for signal detection, is determined by a multiplicative constant  $T$ , ensuring that the probability of false alarm  $P_{FA}$  remains at a predefined minimum level. Hence, the threshold equals the product of  $T$  computed from the designated  $P_{FA}$  and the real-time estimated noise power  $X$ , which varies with the environmental conditions.

Fig I-11 illustrates the CFAR detection method involves serially processing samples from the quadratic detector through a shift register comprising  $N_c + 1$  cells. Among these cells,  $N_c$  reference cells  $Z_i$  ( $i = 1, \dots, N_c$ ) capture outputs from the non-coherent detector corresponding to various potential offsets (phases) of the PN sequence. The statistic  $X$  is then derived from the processing of these reference cells. The initial cell, labeled  $Z_0$  and referred to as the *cell under test (CUT)*, signifies the detector output linked to the phase of the PN sequence being tested.

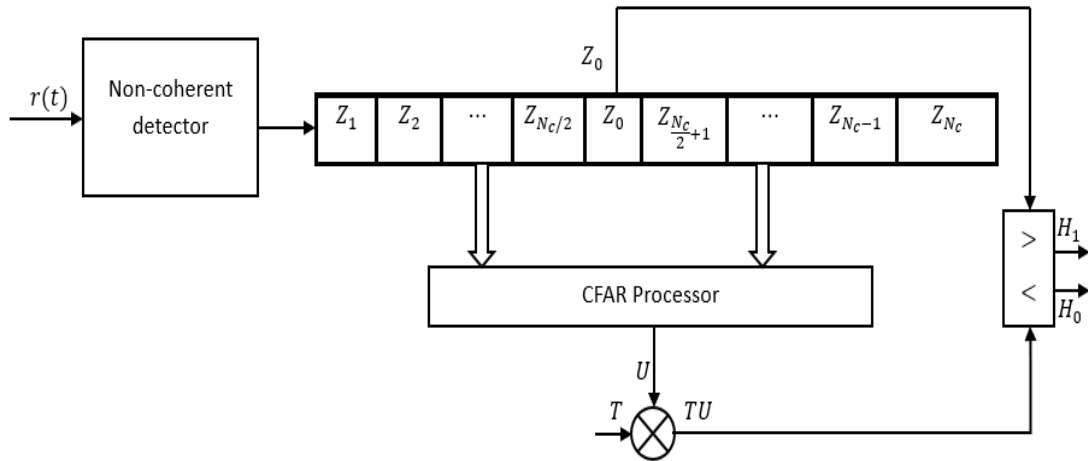


**Fig.I-11:** Block diagram of an adaptive detection system.

When  $Z_0$  surpasses the adaptive threshold, it indicates synchronization between the locally generated PN sequence and the received one. Consequently, the tracking loop is engaged to refine synchronization between both PN sequences for decoding received information accurately.

Conversely, when  $Z_0$  falls below the adaptive threshold, this signifies a lack of synchronization between the received PN code phase and the locally generated one. Consequently, the local PN code is temporally delayed to explore alternative cells.

Several continuous false alarm rate (CFAR) techniques have been used for obtaining the DS/CDMA code to combat change and instability in detection probability ( $P_d$ ) and false alarm probability (PFA). Here are some CFAR detectors used in the field of detection that were later applied to the acquisition of PN sequences in DS/CDMA systems.

**I-12-1 CA-CFAR:**

Finn and Johnson proposed this detector. This algorithm estimates the noise power in real-time, which is equal to the sum or arithmetic mean of samples within the reference window (see Fig I-12).

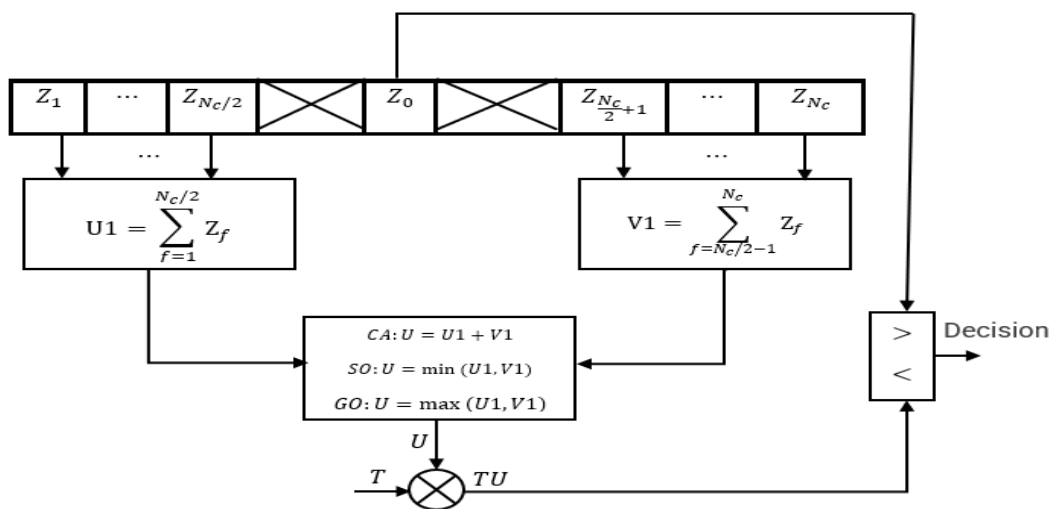


**Fig.I-12:** Block diagram of conventional CFAR detectors.

### I-12-2 GO-CFAR:

Hansen and Sawyers proposed this detector. This algorithm uses the maximum of the sums of outputs from two windows (upstream and downstream) located on both sides of the cell under test. The goal of this improvement is to correct the masking effect [5].

### I-12-3 OS-CFAR:

Rohling proposed the OS-CFAR (Order Statistics) detector, in which the samples from reference cells are ordered in ascending order, and the noise power is taken equal to the  $k^{\text{th}}$  sample. This rank is chosen to maximize the probability of detection (see Fig I-13). [5].

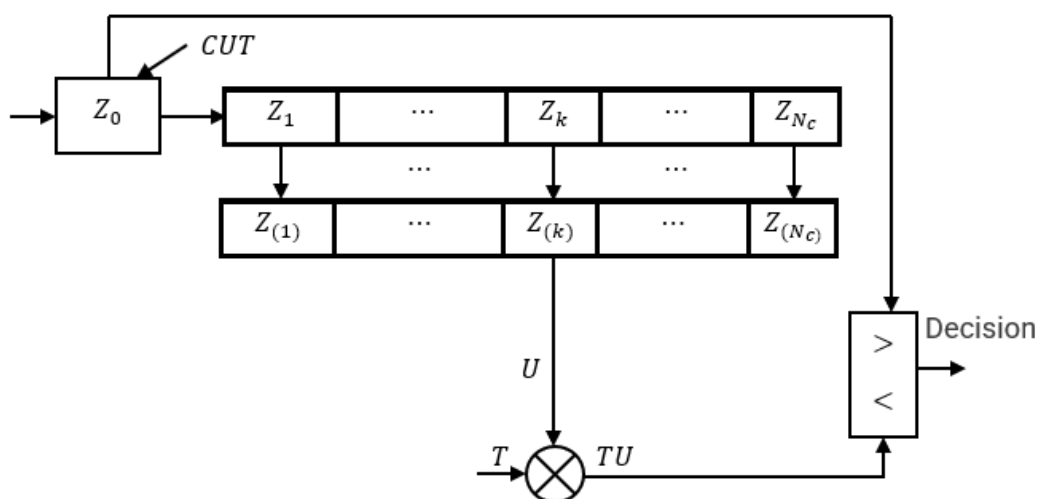


**Fig.I-13:** Functional diagram of the detector OS-CFAR.

### I-12-4 CMLD-CFAR:

Rickard and Dillard proposed the CMLD (Censored Mean Level Detector). The principle of this detector is to estimate the noise level by calculating the average of uncensored cells after censoring cells containing replicas of signals from multipath fading. The outputs of the reference cells are ranked based on their magnitudes in ascending order after censoring  $k$  interference cells. The remaining cells are collected to obtain an estimate of the noise level. The adaptive threshold value is determined through a multiplier  $T$  to obtain the desired probability of false alarm (see Fig I-14) .

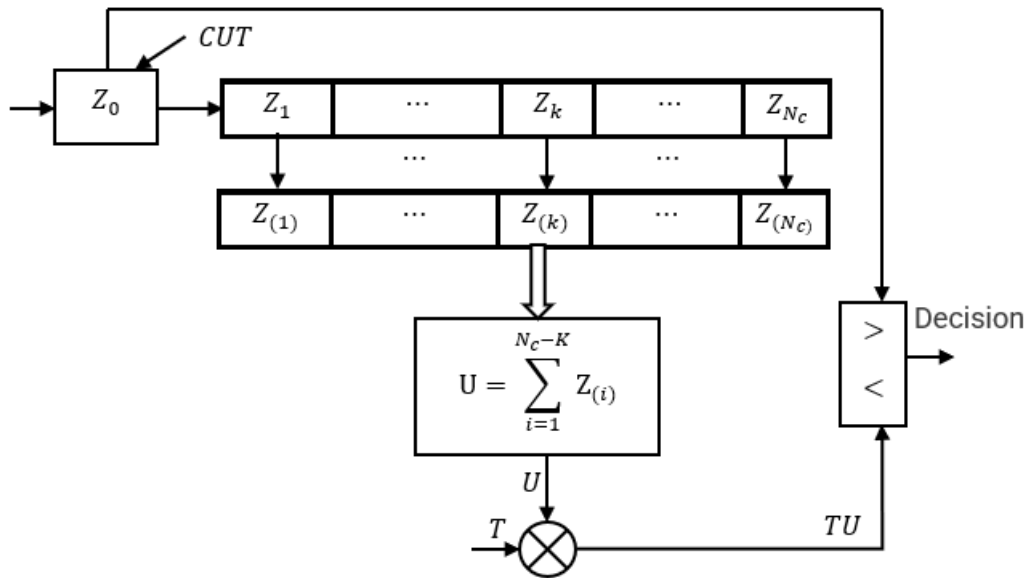


**Fig.I-14:** Block diagram of the detector CMLD-CFAR.

**I-12-5 TM-CFAR:**

The Trimmed Mean CFAR (TM-CFAR) detector has been presented as a hybrid between CA, OS-, and CMLD-CFAR. In this detector, the smallest and largest noise samples are censored, and the estimation of the noise level is obtained from the remaining noise samples (see Fig I-15). [7].

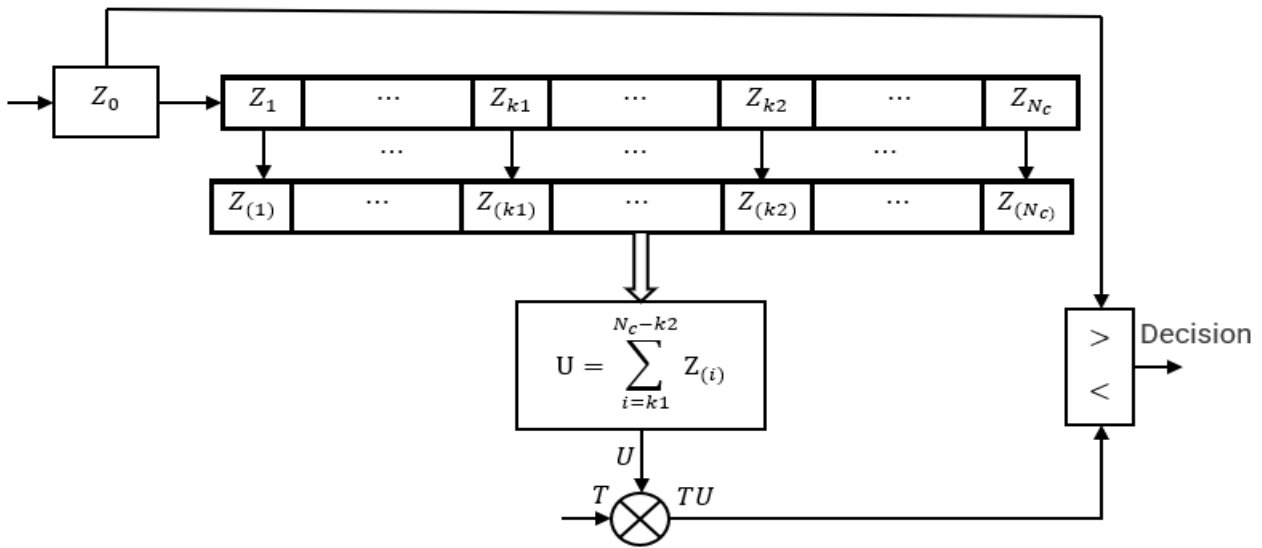


**Fig.I-15:** Functional diagram of the detector TM-CFAR.

**I-12-6 ATM-CFAR:**

In wireless communication systems, the type of environment in which the communication process takes place is crucial. The multipath environment affects the transmitted signal, as it often reflects off buildings, trees, and terrain in the environment, or may cause delay between users.

For this reason, researchers found that each detector among those proposed previously had a relative error that could lead to a flaw in signal detection. Consequently, Sofwan and Barkat proposed a new



algorithm called ATM CFAR (Automatic Trimmed-Mean CFAR), which is one of the most efficient detection algorithms in non-homogeneous environments [8].

### **I-13 Conclusion:**

In this chapter, we have presented the multiplexing techniques used in mobile radio systems. The principle of direct sequence spread spectrum is detailed, by describing its main advantages and disadvantages. We have also mentioned the principle of PN code spreading. Then, we introduced the principle of initial acquisition of the PN sequence and the different search strategies.

Finally, we have provided some types of CFAR detectors applied in PN sequence acquisition problems in DS/CDMA systems.

**Chapter II:**  
**Description of Neural Network ATM-  
CFAR Detector.**

**II-1 Introduction**

In the realm of wireless communication, the efficient acquisition and synchronization of signals is paramount, particularly in environments plagued by noise and interference. The proposed system outlined in this chapter leverages a combination of automatic trimmed-mean constant false alarm rate (ATM-CFAR) detection and convolutional neural networks MLP(Multi-Layer Perceptron) to enhance the adaptive acquisition of pseudo-noise (PN) sequences. This innovative approach not only improves the detection accuracy in multipath environments but also dynamically adjusts to varying signal conditions, thereby ensuring robust performance. The system's architecture encompasses key processes such as signal correlation, neural network-based feature extraction, adaptive threshold setting, and iterative synchronization adjustments, all aimed at maintaining optimal signal acquisition.

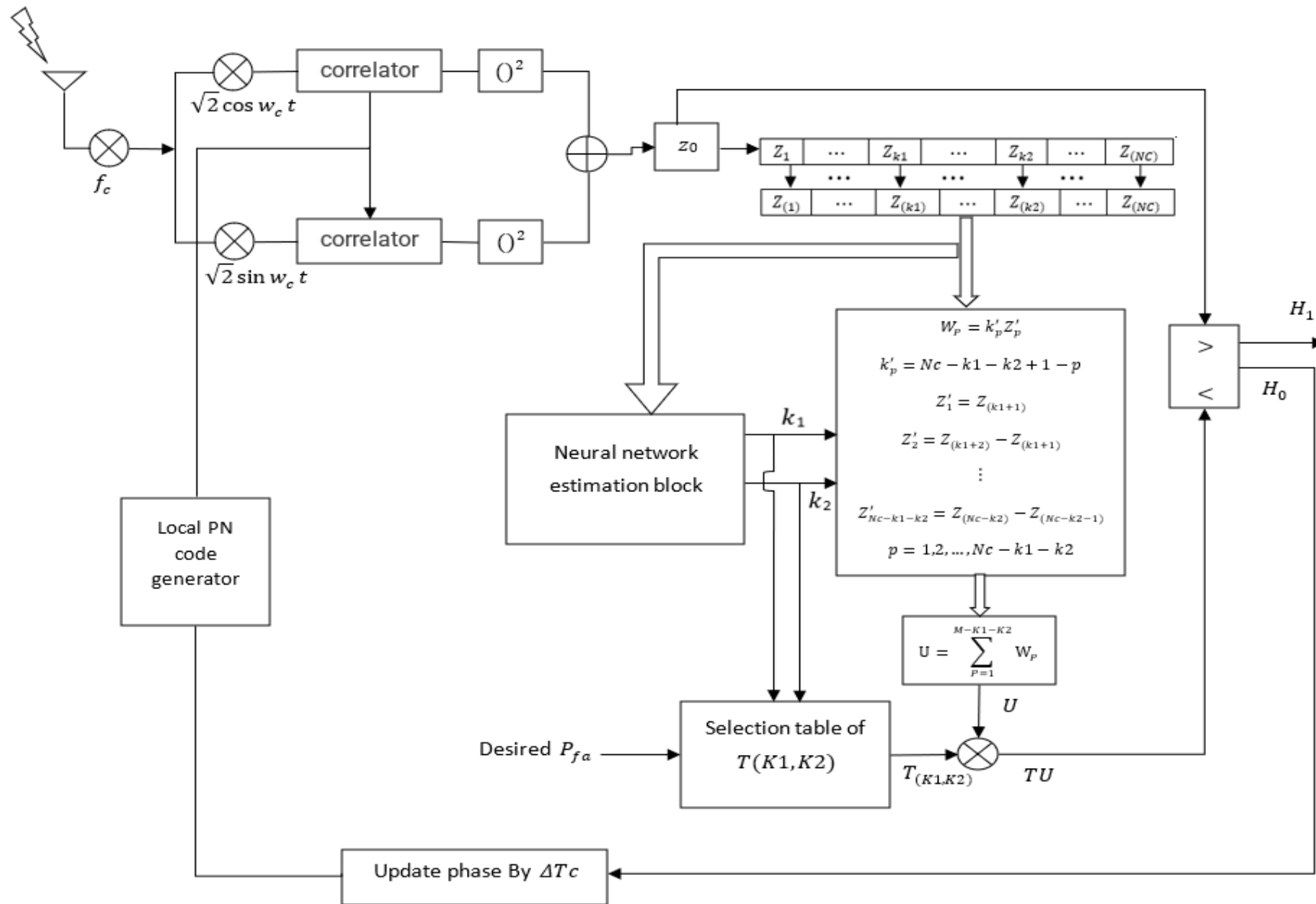


Fig.II-1: Scheme of the proposed system.

## II-2 Application of ATM-CFAR to adaptive PN sequence acquisition:

### II-2-1 Description of the proposed system:

The block diagram of the proposed system is shown in Figure II-1. The diagram of the proposed system outlines a comprehensive signal detection and synchronization mechanism tailored to a communication system involving a single user. This process starts when the antenna receives the input signal. This signal is then mixed with the local oscillator signals  $\sqrt{2} \cos(w_c t)$  and  $\sqrt{2} \sin(w_c t)$  to produce in-phase ( $I$ ) and quadrature ( $Q$ ) components, respectively. These components are directed through correlators to the filter and enhance certain aspects of the signal.

The squared output from the correlator generates a signal  $Z_i$  that acts as an input to the neural network estimation block, which in this case, is an *MLP* (Multi-Layer Perceptron). The *MLP* processes these squared signals through multiple layers to extract important features from the signals. These features are critical for estimating the adaptive thresholds required for accurate target detection. Based on the *MLP*'s output, values for  $(K_1)$  and  $(K_2)$  are determined. They are then used to reference a selection table to set the appropriate adaptive threshold  $T(K_1, K_2)$ .

Following the estimation, the system calculates a series of weighted sums  $W_p$  using the correlator output  $Z'_p$ . These weights are summed to produce the value  $U$ , which is a key factor in the decision-making process. The system then compares  $Z_0$  against the adaptive threshold  $UT(K_1, K_2)$ .  $U$  to determine the presence ( $H_1$ ) or absence ( $H_0$ ) of the signal. If the value  $Z_0$  exceeds the adaptive threshold, the hypothesis  $H_1$  is declared, indicating that signal acquisition was successful. This will trigger the activation of the tracking loop to stay in sync. Conversely, if  $Z_0$  does not exceed the threshold, then the hypothesis  $H_0$  is declared, which means there is no signal acquisition. In this scenario, the system re-initializes the process by adjusting the phase of the local PN code generator with  $\Delta T_c$  to ensure that the PN code is properly aligned for subsequent signal detection attempts.

This cycle of correlation, parameter estimation, summation, comparison, and phase adjustment allow the system to continuously adapt and increase the possibility of accurate detection even in the presence of noise and interference. The integration of neural networks and adaptive threshold mechanisms for input parameter estimation provides robustness and flexibility. The system responds dynamically to changing signal conditions, and improves performance in signal acquisition. It allows you to maintain a high performance through the use of high-speed [9-11].

### II-3 System description and problem formulation:

The communication system model under consideration involves  $D$  users from simultaneous transmitters; with the first user regarded as the initial synchronization point whose performance is the subject of

investigation. Fig.II-1 depicts the block diagram of the proposed communication system model. The transmitted signal of the  $i^{\text{th}}$  user is expressed as:

$$s_i(t) = \sqrt{2P_{T_i}} b_i(t) c_i \cos(\omega_c t + \xi_i) \quad (\text{II -1})$$

Where  $P_{T_i}$  represents the transmitted power of the  $i^{\text{th}}$  signal,  $b_i$  is the data waveform,  $c_i$  is the spreading sequence,  $\omega_c$  is the angular carrier frequency, and  $\xi_i$  is the phase of the  $i^{\text{th}}$  modulator from the transmitter. At the onset of each transmission, the transmitter emits a phase-coded carrier without data modulation to aid initial synchronization [12, 13].

Therefore, for simplicity, we assume that there is no data modulation on the initial synchronization signals. The user signals traverse through a communication channel assumed to be a Rayleigh fading multipath channel. The output undergoes ATM-CFAR (Automatic Trimmed-Mean Constant False Alarm Rate) processing to make a final decision regarding acquisition.

### II-3-1 Received signal model:

The communication channel model considered in this work consists of  $L$  tapped delay lines with a tap spacing of one chip that correspond to the number of resolvable multipath with amplitudes  $a_{il}$  and phases  $\alpha_{il}$ ,  $i = 1, \dots, D, l = 0, \dots, L - 1$ , where  $a_{il}$  is Rayleigh random variable and  $\xi_{il}$  is uniform random variable over  $[0, 2\pi]$ . We assume that the fading amplitude is constant during an observation interval but changes from one to another. Moreover, we normalize the total fading power in all resolvable paths to unity. The average fading power in each path is defined as [14]:

$$E[\alpha_{il}^2] = \frac{1 - \exp(-\mu)}{1 - \exp(-\mu L)} \exp(-l\mu),$$

$$l = 0, 1, 2, \dots, L - 1; \mu \neq 0 \quad (\text{II -2})$$

where  $E[\cdot]$  is the statistical expectation and (II -2) is the exponential decay rate of the diffuse power in each path. The probability density function (pdf) of the distributed Rayleigh random variables  $\alpha_{il}$  is given .

$$f_{\alpha_{il}}(x) = 2x/\psi_{il} \exp(-x^2/\psi_{il}), \quad x \geq 0 \quad (\text{II -3})$$

Where,  $\psi_{il} = E[x_{il}^2]$ ,  $i = 1, \dots, D$ , and  $l = 0, \dots, L - 1$ . The receiving antenna is a linear array of identical elements spaced  $d$  apart, where  $d = 0.5\lambda_c$  and  $\lambda_c$  is the wavelength of the carrier transmitted signal.

The received signal consists of the signal from the first user, multiple access interferences (MAIs) from other users, and additive white Gaussian noise (AWGN)  $n(t)$ . Thus, the received signal at an antenna element can be expressed .

$$\begin{aligned}
r(t) = & \sqrt{2P_s} \left\{ \sum_{l=0}^{L-1} \alpha_{1l} b_1(t - \tau_1 - lT_c) c_1(t - \tau_1 - lT_c) \times \cos(\omega_c t + \varphi_{1l}) \exp(-j\pi \sin \theta_s) \right\} \\
& + \left\{ \sum_{i=2}^D \sqrt{2P_{I_{i-1}}} \sum_{l=0}^{L-1} \alpha_{il} b_i(t - \tau_i - lT_c) c_i(t - \tau_i - lT_c) \right. \\
& \left. \times \cos(\omega_c t + \varphi_{il}) \exp(-j\pi \sin \theta_{i-1}) \right\} + n(t):
\end{aligned}
\tag{II-4}$$

Where:

$P_s$  : Received signal power of the first user.

$P_{I_{i-1}}$  : Received signal power of the interfering user  $i - 1$ .

$\tau_i$  : Relative time delay in the asynchronous communication channel model.

$\varphi_{il} = \xi_i - \xi_{il} - \omega_c(\tau_i + lT_c)$  : Phase in the demodulator of the receiver for user  $i$  and path  $l$ , which  $i = 2, 3, \dots, D$ ,  $l = 0, 1, \dots, L - 1$ .

$T_c$  : Chip duration.

$\theta_s$  : DOA angle if the first user signal.

$\theta_{i-1}$  : DOA angle of the interfering user  $i - 1$

### II-3-2 Correlator:

The correlator corresponding to the single antenna element is depicted in Figure 2. The baseband signal  $r^{(t')}(t)$  at this correlator can be expressed as follows:

$$\begin{aligned}
r^{(t')}(t) = & 2\sqrt{P_s} \left\{ \sum_{l=0}^{L-1} \alpha_{1l} c_1(t - \tau_1 - lT_c) \cos(\omega_c t + \varphi_{1l}) \times \cos(\omega_c t) \right\} \\
& + 2 \left\{ \sum_{i=2}^D \sqrt{P_{I_{i-1}}} \sum_{l=0}^{L-1} \alpha_{il} c_i(t - \tau_i - lT_c) \times \cos(\omega_c t + \varphi_{il}) \cos(\omega_c t) \right\} + n(t)
\end{aligned}
\tag{II-5}$$

The in-phase and quadrature phase ( $I - Q$ ) parts of the correlator are multiplied by the locally generated pseudo-noise  $PN$  code  $c(t - jcT_c/2)$ , where  $jc = 0.1, \dots, Nc$  ( $Nc$  denotes the reference window size of the Constant False Alarm Rate (CFAR) processor). These components are then integrated over a dwell time

interval  $\tau_D = NT_C$  s, where  $N$  is an integer representing the correlation length, resulting in the  $I$  and  $Q$  branch components  $Y^I$  and  $Y^Q$ , respectively.

Subsequently, the output  $Y_m$  from each branch of the correlator comprises the first user signal component, the Multiple Access Interference  $MAI$ , and the Additive White Gaussian Noise  $AWGN$ , which can be mathematically expressed as we observe in Fig.II-2:

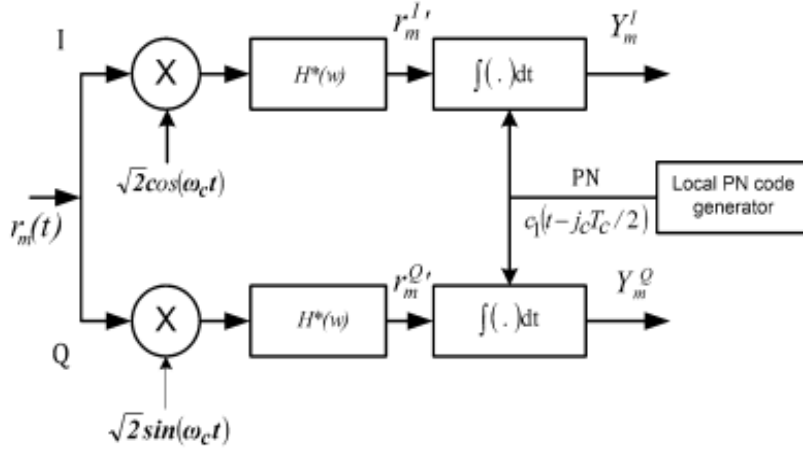


**Fig.II-2:** Correlator consists of in-phase (I) and quadrature-phase (Q) components.

$$Y_m = \left\{ \sum_{l=0}^{L-1} (Y_{Sl}^I + jY_{Sl}^Q) \exp(-j\pi(m-1) \sin \theta_s) \right\} + \left\{ \sum_{i=2}^D \sum_{l=0}^{L-1} (Y_{MAI il}^I + jY_{MAI il}^Q) \times \exp(-j\pi(m-1) \sin \theta_{i-1}) \right\} + n_m \quad (\text{II-6})$$

Where  $Y_{Sl}^I + jY_{Sl}^Q$  denotes  $I-Q$  component of the first user,  $Y_{MAI il}^I + jY_{MAI il}^Q(t)$  denotes  $I-Q$  component of the MAI, and  $n_m(t) = N_m^I(t) + jN_m^Q(t)$  denotes the thermal noise. The in-phase signal component in (II-6) due to the first user is given ,

$$Y_{Sl}^I = \sqrt{P_S} \alpha_{1l} \cos(\varphi_{1l}) [\Delta_1 R_P(j_c, N+1) + (T_c - \Delta_1) R_P(j_c, N)] = \sqrt{P_S R_{Sl}^I} \quad (\text{II-7})$$

where :

$$R_{Sl}^I = \alpha_{1l} \cos(\varphi_{1l}) [\Delta_1 R_P(j_c, N+1) + (T_c - \Delta_1) R_P(j_c, N)] \quad (\text{II-8})$$

$\Delta_1$  represents a random variable uniformly distributed in the interval  $[0, T_c]$ , and  $R_P(j_c, N)$  denotes the code partial autocorrelation function of the initial user. To derive the quadrature phase signal component



of the initial user,  $\cos(\varphi_{il})$  in equation (II-7) is replaced by  $-\sin(\varphi_{il})$ . The in-phase term of multiple access interference  $MAI$  can be defined as

$$Y_{MAIil}^I = \sqrt{P_{l_{i-1}}} \alpha_{il} \cos(\varphi_{il}) \left[ \Delta_l R_P^{(i)}(j_c, N+1) + (T_c - \Delta_l) R_P^{(i)}(j_c, N) \right] = \sqrt{P_{l_{i-1}}} R_{MAIil}^I \quad (\text{II-9})$$

where :

$$R_{MAIil}^I = \alpha_{il} \cos(\varphi_{il}) \left[ \Delta_l R_P^{(i)}(j_c, N+1) + (T_c - \Delta_l) R_P^{(i)}(j_c, N) \right] \quad (\text{II-10})$$

Here,  $R_P^{(i)}(j_c, N)$  represents the code partial cross-correlation between the received sequence of the  $(i-1)^{th}$  user and the locally generated sequence. The  $R_{MAIil}^I$  term reduces the power of the interfering signal exiting the correlator, influenced by a factor of  $R_P^{(i)}(j_c, N)$ . To obtain the quadrature phase signal term of the multiple access interferences  $MAIs$ ,  $\cos(\varphi_{il})$  in equation (II-9) is replaced by  $-\sin(\varphi_{il})$ . The noise term is determined by

$$N_m^I = \int_0^{RT_c} n_m^I c_1(t - jT_c/2) \sqrt{2} \cos(\omega_c t) dt \quad (\text{II-11})$$

The quadrature phase of the noise term is defined by replacing  $\cos(\varphi_{il})$  by  $\sin(\varphi_{il})$ .

### II-3-3 ATM-CFAR detector:

In wireless communication systems, the nature of the environment greatly influences the communication process. The presence of multipath environments can distort transmitted signals, as they may be reflected off buildings, trees, or terrain before reaching the receiver. Additionally, multipath environments can introduce delays between users.

Recognizing the impact of environmental factors on signal detection, researchers observed that the previously proposed detectors exhibited relative errors that could compromise signal detection accuracy. Consequently, Sofwan and Barkat [15] introduced a novel algorithm termed *ATM – CFAR* (Automatic Trimmed-Mean-CFAR), depicted in Figure 2.6. This algorithm represents one of the most recent and effective detection methods designed specifically for non-homogeneous environments. Using this algorithm, the estimation of  $k_1$  and  $k_2$  is made using a statistical method, which called ‘boxplot method’. In the present work the estimation of this two parameters is made using an artificial neural network.

The bloc diagram of the neural network ATM-CFAR provides an overview of the signal detection and synchronization mechanisms of a communication system. It starts with the reception of the input signal  $Z_0$  and is processed through the correlator to produce the outputs  $Z_1$  to  $Z_{N_c}$ . The neural network estimates the parameters  $k_1$  and  $k_2$  that are used to determine the adaptive threshold  $T(K_2, K_1)$  from the selection table. The system uses the modified correlator output to calculate the weighted sums  $W_p$  and then sums them up to produce  $U$ . Then compare the value  $U$  with the threshold  $T \times U$  to determine whether the signal exists ( $H_1$ ) or not ( $H_0$ ). When a signal is detected, the system synchronizes and continues tracking. If no signal

is found, it reinitializes the discovery process. This approach, which integrates neural networks with adaptive thresholds, improves signal detection accuracy under a variety of conditions .

✓ **Input Signal ( $Z_0$ ):**

Input signal is received and processed to extract important information for signal detection.

✓ **Correlator Outputs ( $Z_1, Z_2, \dots, Z_{N_c}$ )**

- The received signal is passed through correlators to produce the values  $Z_1, Z_2, \dots, Z_{N_c}$

✓ **Neural Network Estimation Block :**

- Here, a Multi-Layer Perceptron (MLP) is used to estimate the values  $k_1$  and  $k_2$ .

✓ **Threshold Selection Table  $T(K_1, K_2)$ :**

- This table uses the estimated values  $K_1$  and  $K_2$ , along with the desired probability of false alarm  $P_{fa}$ , to determine the value  $T(K_1, K_2)$ .

✓ **Calculation of Weighted Sums ( $W_p$ ):**

- The weighted sums  $W_p$  are calculated using the modified correlator outputs  $Z'_p$ :

$$W_p = k'_p Z'_p$$

where:

$$k'_p = N_c - k_1 - k_2 + 1 - p$$

$$Z'_1 = Z_{(k_1+1)}$$

$$Z'_2 = Z_{(k_1+2)} - Z_{(k_1+1)}$$

...

$$Z'_{(N_c-k_1-k_2)} = Z_{(N_c-k_2)} - Z_{(N_c-k_2-1)}$$

✓ **Calculation of the Value  $U$ :**

- The value  $U$  is calculated by summing the weighted sums  $W_p$  over the range  $p = 1, 2, \dots, N_c - k_1 - k_2$  :

$$U = \sum_{p=1}^{M=N_c-k_1-k_2} W_p$$

✓ **Décision Making:**

- The value of the cell under test is compared to the threshold multiplied by a constant  $T(K_1, K_2)$  to determine whether the signal is present ( $H_1$ ) or absent ( $H_0$ ). If it exceeds  $U \times T$  the hypothesis  $H_1$  is declared.
- If value of the cell under test is less than or equal to the threshold, the hypothesis  $H_0$  is declared.

## II-3-4 Neural networks:

Neural networks are a program or machine learning model that makes decisions in a manner comparable to the human brain, using processes that mimic the way biological neurons work together to identify phenomena, evaluate options, and draw conclusions.

All neural networks consist of layers of nodes, or artificial neurons: an input layer, one or more hidden layers, and an output layer. Each node connects to another and has an associated weight and threshold. If the output of an individual node is greater than the specified threshold value, that node is enabled, sending the data to the next layer of the network. Otherwise, no data is transmitted to the next layer.

Neural networks rely on training data to learn and improve their accuracy over time. Once they reach an optimal level of accuracy, they are powerful allies in the fields of computing and artificial intelligence, which allow us to classify and group data at high speed. A speech or image recognition task that requires hours of research from a human expert can be completed in minutes. Google's search algorithm is one of the best-known examples of neural networks. Among our types of neural networks there are:

### II-3-4-1 MLP network:

A multi-Layer perceptron (MLP) network, is a directed artificial neural network (as its name suggests) consisting of one intermediate layer called input layer, output layer, and hidden layers. **Figure (II.4)** shows an example of a network with  $n$  inputs, 2 hidden layers, and 1 output layer.

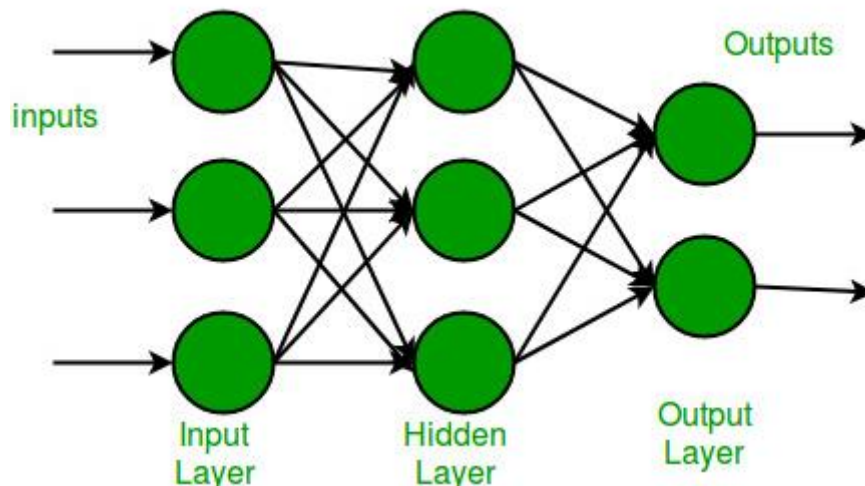


**Fig-II.3:** Example of an MLP network.

The input layer always represents the virtual layer associated with the system's inputs. The neurons in this layer are connected to the outside world and all receive the same input vector (in fact, the neurons in the input layer pass the input without changing). The output of the last layer of neurons always corresponds to the output of the system and provides results. Finally, neurons in other layers (hidden layers) have nothing to do with the outside and are called hidden layers. In general, a multilayer perceptron can have multiple hidden layers and multiple neurons for each layer. In the case of artificial neural networks, training algorithms are often added to the model description. Models without learning are of little interest. In most

current algorithms, the variable changed during training is the weight of the connection. The next section is devoted to the definition and description of the learning algorithm.

## II-4 Learning algorithms:

All the information that can be included in the neural network is in the weight of the synapses. Therefore, training consists of adjusting these weights so that the network can correctly generate the corresponding output for each point in the input space. Thus, learning can be defined as a stage in the development of a neural network in which the behavior of the network changes until the desired behavior is achieved, and can distinguish between three types of learning. In the present work, the supervised learning is used.

### II-4-1 Supervised learning:

The professor provides a data pair (input, corresponding desired output) to the network. The network parameters are adjusted to minimize a certain standard of output error, which is composed by the difference between the actual output of the network and the corresponding desired value (provided by the professor).

### II-5 Backpropagation algorithm:

Using only input/output data, the back propagation algorithm changed the synaptic coefficient ( $w_i$ ) of the network in the opposite direction of the error reference gradient, removed the learning example ( $x_i, y_i$ ) at each iteration, and changed the new estimate of the synaptic weight  $w_i$ . This iteration consists of 2 phases:

✓ **Propagation:** At each iteration, the elements of the training set are introduced through the input layer. Network outputs are evaluated layer by layer, from input to output.

✓ **Backpropagation:** This step is similar to the previous step. However, the calculations are done in the opposite direction (from output to input). At the output of the network, a performance criterion  $E$  is formed according to the actual system output and its desired value. Then evaluate the gradient of  $E$  for different weights starting from the output layer and returning to the input layer.

### II-6 Random Search Method (Monte Carlo Method):

This is the simplest stochastic method. This method consists of drawing a random solution at each iteration. At this point the objective function  $f$  is evaluated. The new value is compared with the previous value. If it is better than the previous one, this value is recorded with the corresponding solution. And the process continues. Otherwise, it returns to the previous point and starts the process again until the stop condition is reached (see Fig.II-4).

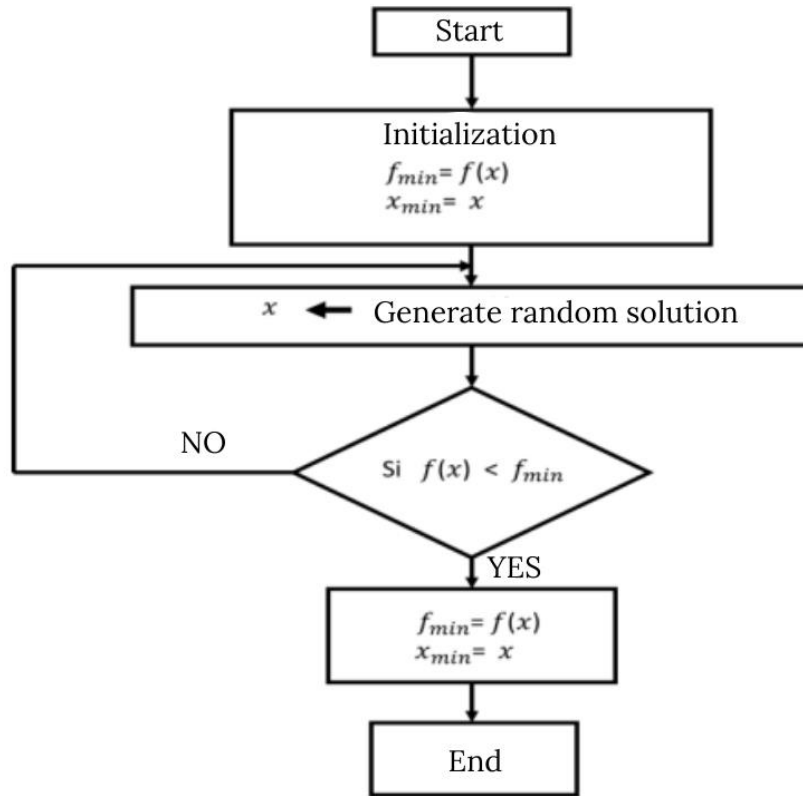


**Fig.II-4:** Random Search Algorithm.

## II-7 Analysis of the proposed system:

### II-7-1 Decision variables:

The received signal is then processed by the in-phase and quadrature phase channels, assuming a correlated chi-square signal with two degrees of freedom embedded in Rayleigh fading channel, the probability density function “pdf” of the hypothesis  $H_1$ ,  $H_1(z/H_1)$ , in the output of each non-coherent detector can be expressed as

$$f_z(z|H_1) = \frac{1}{1+\mu} \exp\left(-\frac{z}{1+\mu}\right), \quad z \geq 0 \quad (\text{II} - 31)$$

where  $\mu$  denotes the average signal to noise ratio (SNR), and the pdf of the sample  $H_0$  is

Under assumption  $H_0$  :

$$f_z(z|H_0) = \exp(-z), \quad z \geq 0 \quad (\text{II} - 32)$$

Using the ATM-CFAR, the reference cells of each AD are ranked firstly in ascending order according to their magnitude to form the ordered samples

$$Z(1) \leq Z(2) \leq \dots \leq Z(N_c) \quad (\text{II-31})$$

### II-7-2 Detection and false alarm probabilities:

The performance of this system can be evaluated through the probability of false alarm  $P_{fa}$  and the probability of detection  $P_d$ . The probability of false alarm in this scenario is determined as follows :

$$P_{fa} = \prod_{i=1}^{N-T_1-T_2} M_{V_i}(T) \quad (II-34)$$

Where,

$$M_{V_1}(T) = \frac{N!}{T_1!(N-T_1-1)!(N-T_1-T_2)} \times \sum_{j=0}^{T_1} \frac{\binom{T_1}{j} (-1)^{T_1-j}}{\frac{N-j}{(N-T_1-T_2)} + T} \quad (II-35)$$

And  $M_{V_i}(T) = \frac{a_i}{a_i+T}$ ,  $i = 2, \dots, N - T_1 - T_2$ .

Where,  $a_i = (N - T_1 - i + 1)(N - T_1 - T_2 - i + 1)$ .

The detection probability  $p_d$  is obtained by replacing  $T$  with  $T/(1 + \mu)$  in (II-34) where  $\mu$  is the signal to noise ratio.

### II-7-3 Mean acquisition time:

The effectiveness of this system can be evaluated using the average acquisition time, which is expressed in terms of  $P_d$  and  $P_{fa}$ . It is represented as follows :

$$\overline{T}_{acq} \approx \frac{(2 - p_d) + (1 + KP_{fa})}{2p_d} (qRT_c) \quad (II-36)$$

With:

- $K$  : represents the penalty time associated with a false alarm.
- $R$  : denotes the partial correlation length.
- $q$  : is the period of the PN sequence.
- $T_c$ : represents the duration of a chip in the PN sequence.

### II-8 Conclusion:

In summary, the integration of ATM-CFAR detection with convolutional neural networks for adaptive PN sequence acquisition presents a significant advancement in communication systems. This method enhances the system's ability to detect and synchronize signals amidst challenging conditions, including multipath interference and noise. The use of neural networks for adaptive threshold estimation provides a flexible and robust mechanism for real-time signal processing. The iterative process of correlation, estimation, summation, and threshold comparison ensures continuous adaptation and high detection accuracy. As a result, this system holds promise for improving the performance of wireless communication networks, particularly in non-homogeneous and dynamic environments, thereby contributing to more reliable and efficient communication technologies.

# **Chapter III:**

## **Results and Discussions**

### III-1 Introduction :

In this chapter, we simulate the Monte Carlo method and the ANN network using MATLAB to investigate the influence of various parameters such as false alarm probability ( $Pfa$ ), partial correlation length ( $N$ ), power ratio ( $\rho$ ), and the number of interfering cells ( $r$ ) on detection probability ( $Pd$ ) and acquisition time ( $Taq$ ). This analysis aims to compare the impact of these parameters on the improvement of results.

### III.2 Results and discussions :

In this section, we check the detection probability  $pd$  and  $taq$  , taking into account the following assumptions:

- 1- False alarm rate values  $Pfa=10^{-3}$  ,  $10^{-4}$  and  $10^{-5}$ .
- 2- The number of reference cells  $Nc=32$ .
- 3- The number of interference cells  $r=2, 6$  and  $10$ .
- 4- The partial correlation length  $N=64, 96$  and  $128$ .
- 5- The ratio of the interference power to the signal power  $\rho=0.3, 1$  and  $3$ .

After many attempts, the ANN was selected based on the smallest error in the output and network (see Fig.III-1)

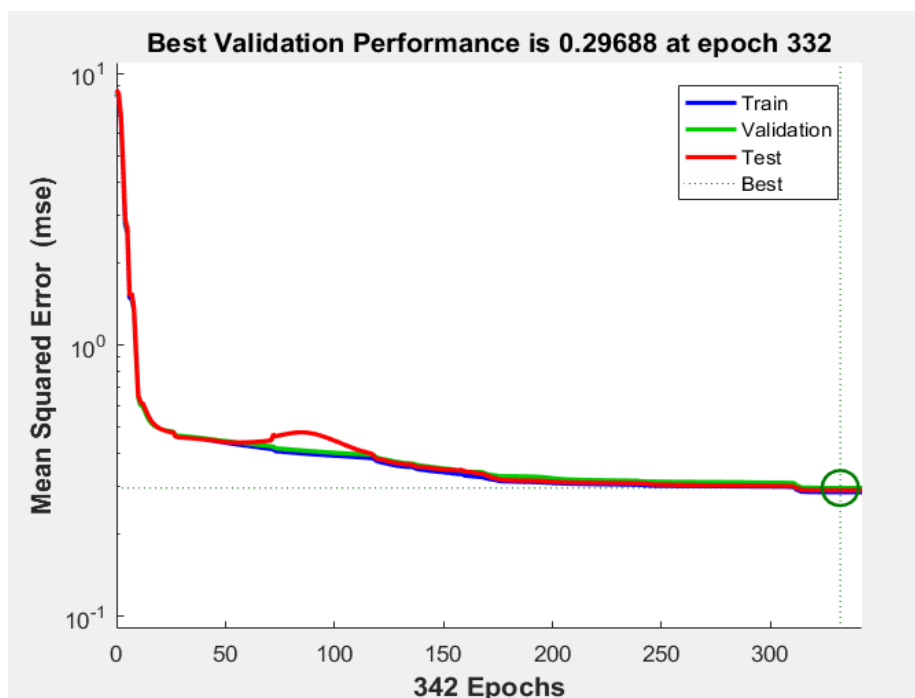


**Fig.III-1:** Database training using the MLP network.



### III.2.1 Effect of interfering cell number ( $r$ ):

Results obtained for the following parameters:

- $r=2, 6, 10$  ;  $N_c=32$  ;  $N=64$  ;  $\rho=1$  ;  $P_{fa}=10^{-4}$

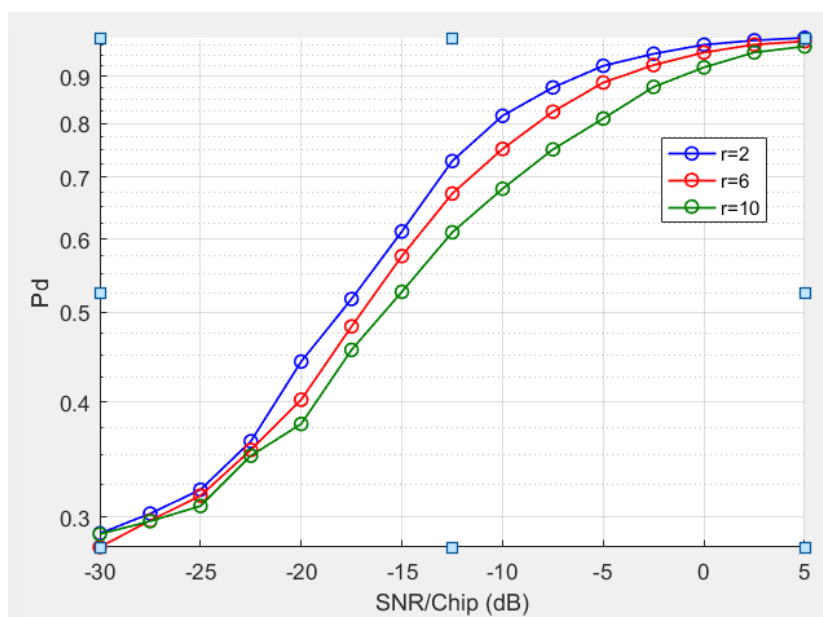


**Fig.III-2:** Probability of detection according to the (SNR/Chip) for different interfering cell numbers ( $r$ ).

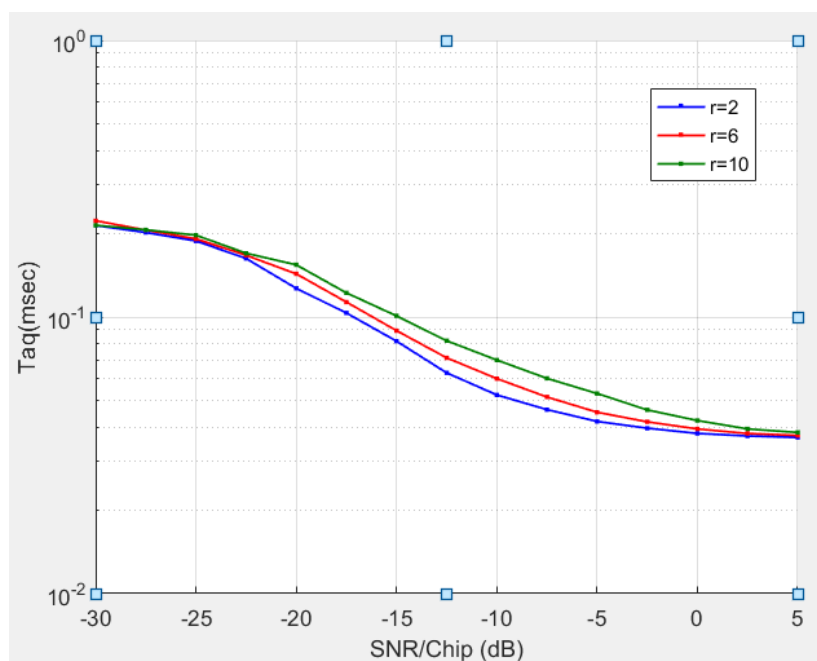


**Fig.III-3:** Time of acquisition according to the (SNR/Chip) for different interfering cell numbers ( $r$ ).

In Fig(III.2) : From the graph, it can be observed that decreasing  $r$  improves the signal detection performance (increases the value of  $P_d$ ) at various levels of Signal-to-Noise Ratio per Chip (SNR/Chip). When  $r$  is smaller ( $r=2$ ), the detection performance is better compared to larger  $r$  values. This means that decreasing  $r$  correctly enhances signal detection over a wide range of SNR values.

In Fig (III.3): From the second graph, it can be observed that decreasing  $r$  slightly improves the acquisition time  $T_{aq}$  at various levels of Signal-to-Noise Ratio per Chip (SNR/Chip). We notice that  $T_{aq}$  decreases significantly with a decrease in  $r$  at low SNR values (from -30 dB to -20 dB). After that, the differences between the three  $r$  (2, 6, 10) become less noticeable as the SNR increases, with the values converging more closely. Overall, we can say that decreasing  $r$  helps improve detection performance and reduce acquisition time  $T_{aq}$ , especially in high noise conditions (low SNR values).

### III.2.2 Effect of partial correlation length N:

Results obtained for the following parameters:

- $N=64, 96, 128$  ;  $N_c=32$  ;  $\rho=1$  ;  $r=6$  ;  $P_{fa}=10^{-4}$

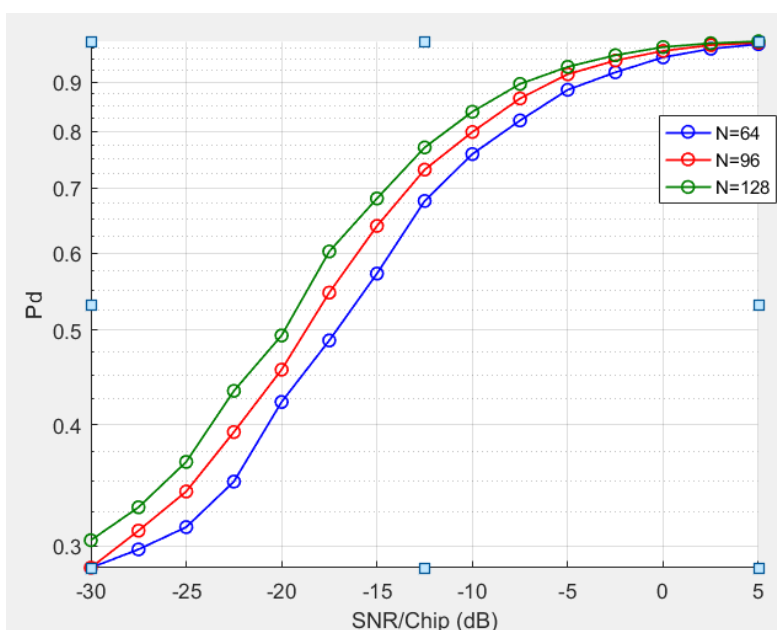


**Fig.III-4:** Probability of detection according to the SNR/Chip for different partial correlation lengths (N).

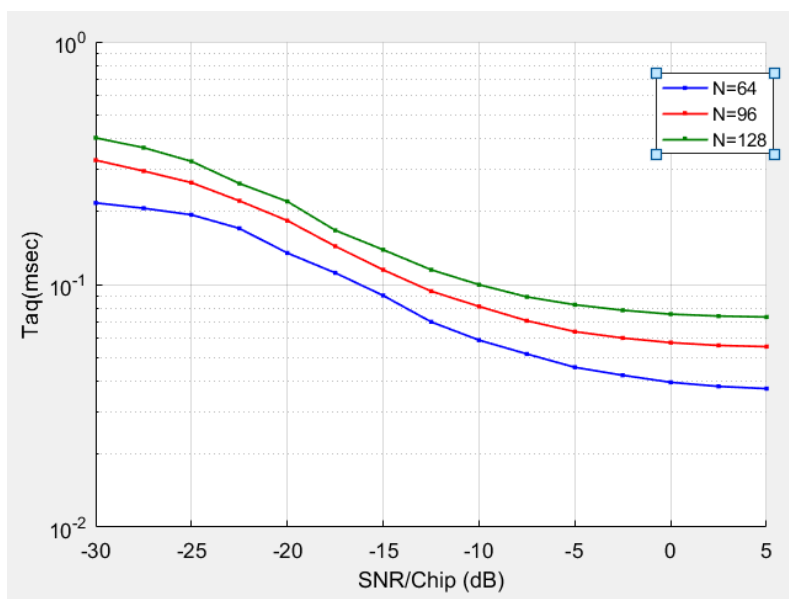


**Fig.III-5:** Time of acquisition according to the SNR/Chip for different partial correlation lengths (N).

In Fig (III.4) : The graph illustrates the effect of the partial correlation length  $N$  on the probability of detection  $Pd$  at various Signal-to-Noise Ratio per Chip (SNR/Chip) values. It is evident from the graph that  $Pd$  improves with the increase of  $N$ .

- (N = 64): At the lowest value of  $N$  (64),  $Pd$  is relatively lower compared to higher values of  $N$  at the same SNR. This indicates that detection performance is relatively weaker.
- (N = 96): Increasing  $N$  to 96 improves detection performance, with  $Pd$  being higher for each SNR value compared to the previous case.
- (N = 128): At the highest  $N$  (128), detection performance is the best, showing the highest  $Pd$  across all SNR values.

It is clear that increasing  $N$  enhances the detection performance  $Pd$  at all SNR values, thereby improving the system's ability to detect the signal in the presence of noise and interferences.

In Fig (III.5) : The graph illustrates the effect of  $N$  on the acquisition time  $Taq$  at various Signal-to-Noise Ratio per Chip (SNR/Chip) values. It is evident from the graph that the acquisition time decreases as  $N$  decreases.

- (N = 64): At the lowest  $N$  (64), the acquisition time  $Taq$  is lower, especially at low SNR values. The performance is notably better compared to higher sample counts at the same SNR values.
- (N = 96): Increasing  $N$  to 96 results in a slightly higher acquisition time compared to the previous case, but the performance remains relatively good.
- (N = 128): At the highest  $N$  (128), the acquisition time is the highest among the three cases for the same SNR values, indicating that an increase in  $N$  leads to an increase in the acquisition time.

The graph clearly shows that reducing  $N$  decreases the acquisition time  $Taq$ , meaning that the system can acquire the signal faster with a lower  $N$ .

### III.2.3 Effect of False Alarm Probability (Pfa):

Results obtained for the following parameters:

- $Pfa = 10^{-3}, 10^{-4}, 10^{-5}$  ;  $Nc=32$  ;  $N=64$  ;  $\rho=1$  ;  $r=6$

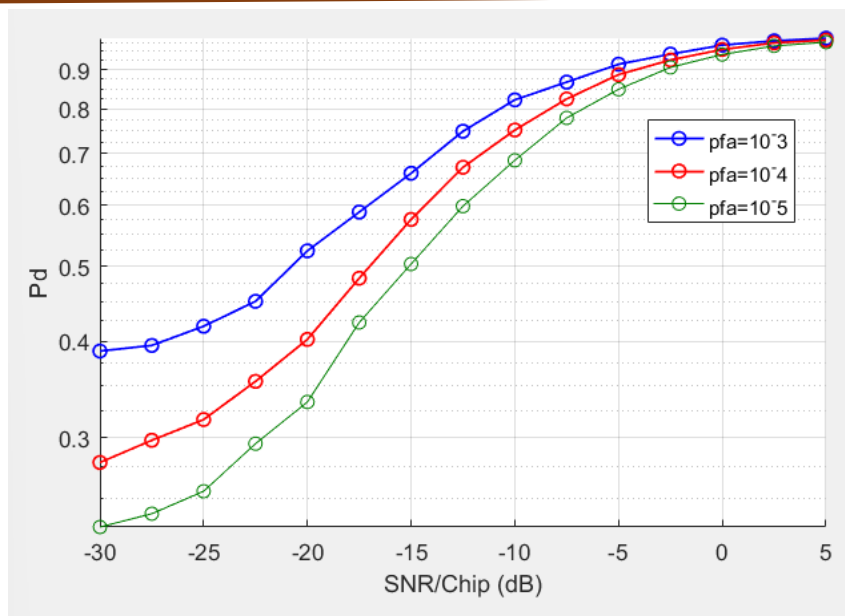


**Fig.III-6:** Probability of detection according to (SNR/Chip) for different false alarm probabilities (Pfa).

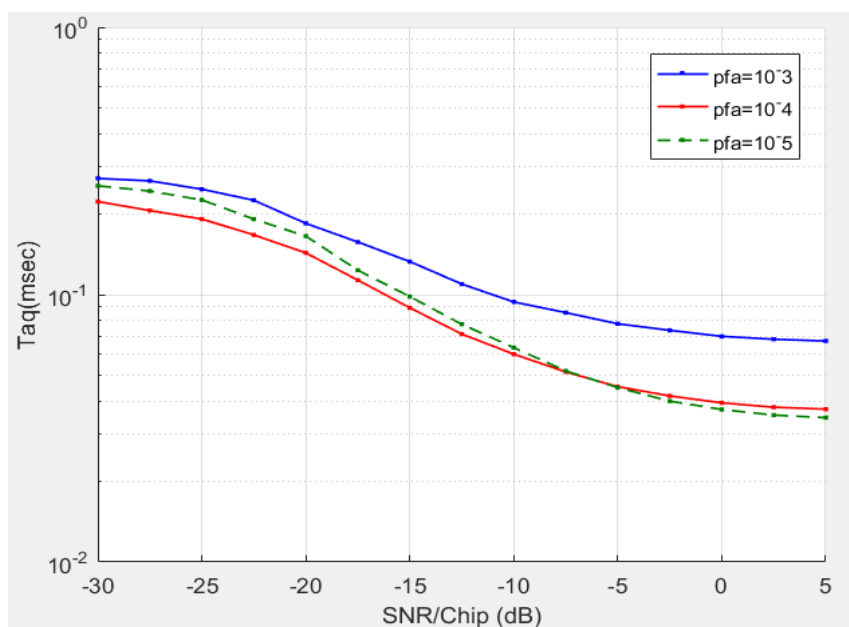


**Fig.III-7:** Time of acquisition according to (SNR/Chip) for different false alarm probabilities (Pfa).

In Fig (III.6): The impact of the false alarm probability ( $Pfa$ ) on the detection probability ( $Pd$ ) is demonstrate. When comparing the three different values of false alarm probability ( $Pfa$ ), the probability of detection ( $Pd$ ) is observed to be higher at smaller  $Pfa$  values  $10^{-3}$  Compared to  $10^{-4}$  and  $10^{-5}$ .

In Fig (III.7) : The graph illustrates the relationship between the Signal-to-Noise Ratio per Chip (SNR/Chip) and the acquisition time  $Taq$  at three different values of the Probability of False Alarm  $Pfa$ , which are  $10^{-3}$ ,  $10^{-4}$ , and  $10^{-5}$ . It is observed that the acquisition time  $Taq$  increases with an increase in the SNR/Chip for all three values of the Probability of False Alarm  $pfa$ . However, at the same SNR/Chip value, the acquisition time  $Taq$  is longer when the Probability of False Alarm  $pfa$  is higher. Therefore, reducing the Probability of False Alarm  $pfa$  can lead to an improvement in the acquisition time  $Taq$ .

### III.2.4 Effect of power ratio ( $\rho$ ):

Results obtained for the following parameters:

- $\rho=0,3,1,3$  ;  $N_c=32$  ;  $N=64$  ;  $r=6$  ;  $P_{fa}=10^{-4}$

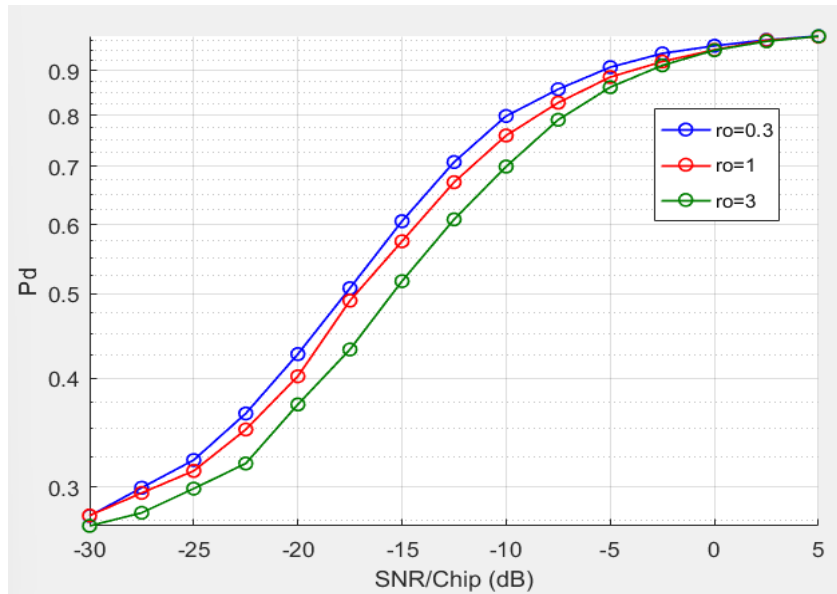


**Fig.III-8:** Probability of detection according to the SNR/Chip for different values of power ratio ( $\rho$ ).

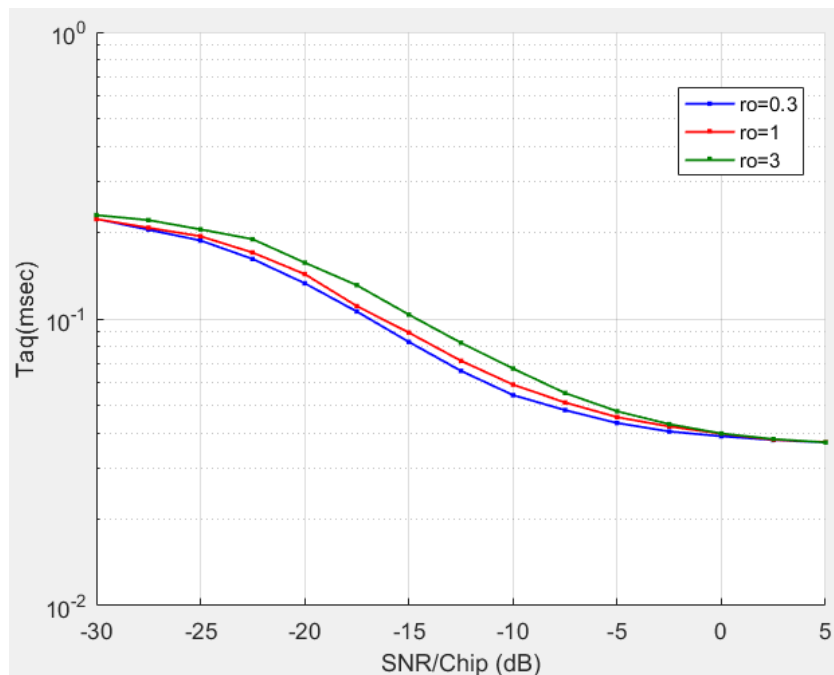


**Fig.III-9:** Time of acquisition according to the SNR/Chip for different values of power ratio ( $\rho$ ).

In Fig (III.8): The graph illustrates the effect of the parameter  $\rho$  on the probability of detection  $P_d$  at various Signal-to-Noise Ratio per Chip (SNR/Chip) values. From the graph, we observe that as  $\rho$  increases, the probability of detection  $P_d$  decreases for the same SNR values. Specifically, when  $\rho=0.3$ , the detection probability is the highest, showing better performance across all SNR values. As  $\rho$  increases to 1 and then to 3,  $P_d$  progressively decreases, indicating that higher  $\rho$  values result in lower detection probabilities. This

suggests that the system's ability to detect the signal diminishes with an increase in  $\rho$ . The detection probability  $P_d$  improves with higher SNR values regardless of  $\rho$ , but for each SNR value, lower  $\rho$  consistently yields better detection performance.

In Fig (III.9): The graph shows the impact of the parameter  $\rho$  on the acquisition time  $T_{aq}$  as a function of SNR/Chip values. As SNR/Chip increases,  $T_{aq}$  decreases significantly for all  $\rho$  values. At high SNR/Chip (0 to 5 dB),  $T_{aq}$  is very low (below 0.01 ms) regardless of  $\rho$ . In the medium range (-10 to 0 dB),  $T_{aq}$  increases with decreasing SNR/Chip, more for higher  $\rho$  values. At low SNR/Chip (-30 to -10 dB),  $T_{aq}$  is markedly higher for larger  $\rho$  values, indicating a significant dependency on  $\rho$  under poor signal conditions, we can conclude that a lower  $\rho$  value (such as 0.3) results in a better performance in terms of acquisition time  $T_{aq}$ , especially under poor signal conditions (low SNR/Chip). When  $\rho$  is above 1,  $T_{aq}$  is generally higher, indicating slower acquisition times. Therefore, a  $\rho$  value of 0.3 is preferable for minimizing acquisition time across various SNR/Chip values.

### III.3 Conclusion :

Based on the analysis of the various figures, it is evident that optimizing system parameters such as  $r$ ,  $N$ ,  $P_{fa}$ , and  $\rho$  significantly impacts both signal detection performance and acquisition time. Decreasing  $r$  enhances detection probability  $P_d$  and reduces acquisition time  $T_{aq}$ , especially in high noise conditions. Increasing the partial correlation length  $N$  improves  $P_d$  but also increases  $T_{aq}$ . Higher  $P_{fa}$  values improve  $P_d$  but result in longer  $T_{aq}$ . Lastly, a lower  $\rho$  yields better  $P_d$  and shorter  $T_{aq}$ , particularly under low SNR conditions. Thus, careful tuning of these parameters can significantly enhance the overall performance of the signal detection system.

# **General Conclusion**

This study thoroughly explored the challenges and solutions associated with PN sequence acquisition in DS/CDMA systems, with a particular focus on the use of adaptive techniques to maintain a constant false alarm rate (CFAR). The primary contribution of this research is the development and evaluation of the ATM-CFAR algorithm, which significantly enhances detection performance in non-homogeneous and degraded environments.

By incorporating an adaptive threshold mechanism, the ATM-CFAR algorithm dynamically adjusts to variations in noise and interference levels using artificial neural network. This adaptability reduces the incidence of false alarms and increases the reliability of initial synchronization processes. Simulations demonstrated that this approach outperforms traditional fixed threshold methods, offering robust performance even in challenging propagation conditions.

The results obtained from this study confirm the critical importance of using adaptive detection techniques in DS/CDMA systems, especially for mobile transmissions where channel conditions can vary significantly. The ATM-CFAR algorithm was shown to effectively enhance the probability of detection ( $P_d$ ) while managing the probability of false alarm ( $P_{fa}$ ), thereby optimizing the overall system performance. Additionally, the algorithm's ability to adapt to varying signal-to-noise ratios ( $SNR$ ) and interference conditions ensures reliable performance in diverse operational scenarios.

The analysis of various system parameters revealed that optimizing these parameters, such as the number of interfering cells ( $r$ ), partial correlation length ( $N$ ), false alarm probability ( $P_{fa}$ ), and power ratio ( $\rho$ ), has a substantial impact on both signal detection performance and acquisition time. For instance, decreasing the number of interfering cells ( $r$ ) enhances detection probability and reduces acquisition time, particularly in high noise conditions. Similarly, increasing the partial correlation length ( $N$ ) improves detection probability but also increases acquisition time. Higher false alarm probabilities ( $P_{fa}$ ) improve detection probability but result in longer acquisition times. Lastly, a lower power ratio ( $\rho$ ) yields better detection probabilities and shorter acquisition times, especially under low  $SNR$  conditions. Thus, careful tuning of these parameters can significantly enhance the overall performance of the signal detection system.

This study also paves the way for future research on improving synchronization algorithms by integrating traditional methods with artificial intelligence approaches, potentially leading to even more optimized performance. The use of neural networks for adaptive threshold estimation offers a flexible and robust mechanism for real-time signal processing, further enhancing the system's ability to detect and synchronize signals in dynamic and multipath environments.

In conclusion, this research makes a significant contribution to the development of more efficient and reliable wireless communication systems by proposing a robust solution for PN sequence acquisition. The



ATM-CFAR algorithm, with its adaptability and improved performance, represents a major advancement in the field of telecommunications, meeting the growing demands for robustness and reliability in modern communication networks. The findings underscore the potential of adaptive detection techniques to significantly enhance the performance of DS/CDMA systems, ensuring more reliable and efficient communication technologies for future applications.

# References

- [1] Aounallah Naceur. « Utilisation des antennes intelligentes dans les systèmes de communications sans fil ». Thèse de Doctorat, Université Djilli Liabes De Sidi Bel Abbes ,2014/2015.
- [2] L. Hacini, Schémas hybrides d'acquisition adaptative de codes PN pour des communications DSSCDMA dans un canal Rayleigh, Thèse de Doctorat, Université Mentouri Constantine, 2012.
- [3] Michel Thériault : Mémoire présenté pour l'obtention du grade de Maître Sciences (M.Sc) UNIVERSITÉ LAVAL QUÉBEC 2005 : Etude des performances d'un système DS-CDMA avec récepteur Rake dans le contexte UWB.
- [4] Ahmad Yehya Fawaz Université Du Québec : Comme exigence partielle de la Maîtrise en génie électrique : Etude comparative des détecteurs ds-cdma dans différents environnements mimo.Octobre 2008.
- [5] BENKRINAH Sabra Thèse doctorat 2018 : La synchronisation CFAR dans les systèmes de communications CDMA.
- [6] G. L. Stüber, Principales of Mobile communication, Springer, 2017. [7] A. Aissaoui, Synchronisation adaptative du code PN dans les systèmes de communication DS/SS, Thèse de Doctorat, Université Mentouri Constantine, 2008.
- [7] N. Alhariqi, M. Barkat and A. Sofwan, "Serial PN Acquisition Using Smart Antenna and Censored Mean Level CFAR adaptive thresholding for à DS/CDMA mobile communication," IEEE 14th International Conference on High Performance Computing and Communications, HPCC, 2012.
- [8] A. Sofwan, M. Barkat and S. A. AlQahtani, "PN Code Acquisition Using Smart Antennas and Adaptive Thresholding for Spread Spectrum Communications," Wireless Networks, Vol. 22, N°.1, pp.223–234, 2016.
- [9] Hu, Y. H. (1993). A Survey of Neural Networks for Signal Processing. *IEEE Transactions on Neural Networks*, 4(4), 570-579. doi:10.1109/72.238329.
- [10] Zhang, Z., & Haykin, S. (1998). Adaptive Signal Detection and Classification. *IEEE Transactions on Signal Processing*, 46(5), 1373-1385. doi:10.1109/78.668819.
- [11] Mengali, U., & D'Andrea, A. N. (1997). Synchronization Techniques for Digital Receivers. *IEEE Communications Magazine*, 35(2), 126-133. doi:10.1109/35.568211.
- [12] Polydoros, A., & Weber, C. (1984). A unified approach to serial search spread-spectrum code acquisition—Part I: General theory. *IEEE Trans. Commun.*, 32, 542–549.

- [13] Lie-Liang, Y., & Hanzo, L. (2001). Serial acquisition of DSCDMA signals in multipath fading mobile channels. *IEEE Trans. Veh. Technol.*, 50, 617–628..
- [14] Rick, R. R., & Milstein, L. B. (1998). Optimal decision strategies for acquisition of spread-spectrum signals in frequency-selective fading channels. *IEEE Trans. Commun.*, 46, 686–694.
- [15] Barkat, M. (2005). *Signal detection and estimation* (2nd ed.). Boston, MA: Artech House.

**Abstract:**

The primary objective of this study is to master and assess the performance of the Adaptive Trimmed mean Mechanism Constant False Alarm Rate (ATM-CFAR) detector. The system under investigation utilizes a straightforward serial search strategy and incorporates an adaptive detector based on multilayer artificial neural networks (ANNs), trained via the backpropagation algorithm. ANNs are computational models inspired by the human brain, capable of recognizing patterns and making decisions. These networks consist of interconnected layers of nodes (neurons) that process input data, learn from it, and improve detection capabilities over time. Our findings underscore the critical role and efficiency of systems employing automatic censoring algorithms in the acquisition process. Moreover, the proposed system demonstrates a superior detection probability, affirming its suitability for advanced applications across diverse technological fields. The study comprehensively explores the integration of neural networks in adaptive detection, highlighting significant improvements in detection capabilities and overall system performance.

**Key words:** Adaptive Trimmed Mean Mechanism Constant False Alarm Rate (ATM-CFAR), artificial neural networks (ANNs), backpropagation algorithm, automatic censoring algorithms, detection probability.

**ملخص:**

الهدف الأساسي من هذه الدراسة هو إتقان وتقييم أداء كاشف آلية المتوسط المعدل التكيفي ذات معدل الإنذار الكاذب الثابت (ATM-CFAR). النظام الذي يتم التحقيق فيه يستخدم استراتيجية بحث تسلسلي بسيطة ويشمل كاشفاً تكيفياً يعتمد على الشبكات العصبية الاصطناعية متعددة الطبقات (ANNs)، المدربة عبر خوارزمية التغذية العكسية. الشبكات العصبية الاصطناعية هي نماذج حسابية مستوحاة من الدماغ البشري، قادرة على التعرف على الأنماط واتخاذ القرارات. تتكون هذه الشبكات من طبقات متصلة من العقد (العصبونات) التي تعالج بيانات الإدخال، وتتعلم منها، وتحسن قدرات الكشف بمرور الوقت. تؤكد نتائجنا على الدور الحاسم والكفاءة للأنظمة التي تستخدم خوارزميات التصفية التلقائية في عملية الاستحواذ. علاوة على ذلك، يظهر النظام المقترح احتمالية كشف فائقة، مما يؤكد ملاءمته للتطبيقات المتقدمة عبر مختلف المجالات التكنولوجية. تستكشف الدراسة بشكل شامل دمج الشبكات العصبية في الكشف التكيفي، مما يبرز التحسينات الكبيرة في قدرات الكشف والأداء العام للنظام.

الكلمات الرئيسية: آلية المتوسط المعدل التكيفي ذات معدل الإنذار الكاذب الثابت (ATM-CFAR)، الشبكات العصبية الاصطناعية (ANNs)، خوارزمية التغذية العكسية، خوارزميات التصفية التلقائية، احتمالية الكشف.

**Résumé:**

L'objectif principal de cette étude est de maîtriser et d'évaluer les performances du détecteur Adaptive Trimmed Mean Mechanism Constant False Alarm Rate (ATM-CFAR). Le système étudié utilise une

stratégie de recherche sérielle simple et intègre un détecteur adaptatif basé sur des réseaux de neurones artificiels multicouches (ANNs), entraînés via l'algorithme de rétropropagation. Les réseaux de neurones artificiels sont des modèles computationnels inspirés par le cerveau humain, capables de reconnaître des motifs et de prendre des décisions. Ces réseaux sont constitués de couches interconnectées de nœuds (neurones) qui traitent les données d'entrée, apprennent de celles-ci et améliorent les capacités de détection au fil du temps. Nos résultats soulignent le rôle crucial et l'efficacité des systèmes utilisant des algorithmes de censure automatique dans le processus d'acquisition. De plus, le système proposé démontre une probabilité de détection supérieure, confirmant son aptitude pour des applications avancées dans divers domaines technologiques. L'étude explore de manière exhaustive l'intégration des réseaux de neurones dans la détection adaptative, mettant en évidence des améliorations significatives des capacités de détection et des performances globales du système.

Mots-clés: Adaptive Trimmed Mean Mechanism Constant False Alarm Rate (ATM-CFAR), réseaux de neurones artificiels (ANNs), algorithme de rétropropagation, algorithmes de censure automatique, probabilité de détection.